READING DISC-BASED BIOASSAYS FOR PROTEIN BIOMARKERS WITH STANDARD COMPUTER DRIVES

by

Miao-Ling (Lily) Ou
B.Sc., Simon Fraser University, 2007

THESIS SUBMITTED IN PARTIAL FULFILLMENT OF
THE REQUIREMENTS FOR THE DEGREE OF

MASTER OF SCIENCE

In the
Department of Chemistry

SIMON FRASER UNIVERSITY

Summer 2011

APPROVAL

Name: **Miao-Ling (Lily) Ou**

Degree: **Master of Science**

Title of Thesis: **Reading Disc-Based Bioassays for Protein Biomarkers with Standard Computer Drives**

Examining Committee:

Chair: **Dr. Paul Li**
Professor, Department of Chemistry

Dr. Hua-Zhong (Hogan) Yu
Senior Supervisor
Professor, Department of Chemistry

Dr. David Vocadlo
Committee Member
Associate Professor, Department of Chemistry

Dr. Ash Parameswaran
Committee Member
Professor, School of Engineering Science

Dr. Tim Storr
Internal Examiner
Assistant Professor, Department of Chemistry

Date Defended/Approved: May 16, 2011

Declaration of
Partial Copyright Licence

ABSTRACT

Current methods of biomedical diagnosis are often limited to centralized laboratories due to the requirement of bulky, sophisticated instruments. This thesis project has the goal of improving the sensitivity and accessibility of existing diagnostic tools for protein biomarkers by combining the popular enzyme-linked immunosorbent assay (ELISA) method with the compact disc (CD) technology. The polycarbonate base of a CD can be activated with a mild UV/ozone treatment, and its feasibility for preparing and running DNA hybridization assays has been demonstrated. Commercially available CD-quality analysis software is capable of quantifying the biotin-streptavidin binding reaction, a model system for biomedical diagnostic assays. After the validation of the CD-based assay preparation and reading protocol, the detection of a blood-borne cancer marker, CA215, has been explored. The sensitivity of the technique is comparable to the conventional ELISA assay, and it undoubtedly improves the accessibility and reduces the cost of current biomedical tests.

Keywords: CD; error determination; CD-quality analysis; silver enhancement; ELISA; biomarker.

ACKNOWLEDGEMENTS

I would like to express my deepest gratitude to my senior supervisor, Dr. Hua-Zhong (Hogan) Yu, for giving me the opportunity to be involved in this research project. Under his guidance, I have learned many valuable research skills. I would also like to thank my committee members Dr. D. Vocadlo and Dr. A. Parameswaran for giving me advices and suggestions for the research. I would like to express my appreciation to Dr. T. Storr for taking the time to be the internal examiner of this thesis project. I would like to acknowledge the funding agencies, the Natural Sciences and Engineering Research Council, Michael Smith Foundation for Health Research, and Simon Fraser University for their financial supports.

My special thanks go to Dr. Y. Li, Dr. H. Wang, Dr. B. Ge, and Dr. H. Yang for their valuable advices for the project. In addition to their precious suggestions for the project, Dr. Y. Li has taught me how to perform the experiments and Dr. H. Wang has helped me with the experiments. I am grateful for their help. I would also like to thank past and present members of the Yu laboratory for their friendship and support.

TABLE OF CONTENTS

LIST OF FIGURES

LIST OF TABLES

GLOSSARY

AFM	Atomic force microscopy
BD	Blu-ray disc
BSA	Bovine serum albumin
CA215	Cancer antigen 215
CD	Compact disc
CD-R	Compact disc recordable
CD-ROM	Compact disc read-only memory
CIRC	Cross interleave Reed-Solomon code
DNA	Deoxyribonucleic acid
ssDNA	Single stranded deoxyribonucleic acid
DTT	Dithiothreitol
DVD	Digital versatile disc
EDC	1-ethyl-3-(3’-dimethylaminopropyl)-carbodiimide
ELISA	Enzyme-linked immunosorbent assay
HD DVD	High-definition digital versatile disc
IgG	Immunoglobulin G
LBA	Logical block address
MES	2-(N-morpholino)ethanesulfonic acid
NHS	N-hydroxysuccinimide

ODR	Optical darkness ratio
PBS	Phosphate buffered saline
PC	Polycarbonate
PCR	Polymerase chain reaction
PDMS	Poly(dimethylsiloxane)
PET	Polyethylene terephthalate
PMMA	Poly(methylmethacrylate)
POC	Point-of-care
PS	Polystyrene
R^2	Correlation of determination
rms	Root-mean-square
SAM	Self-assembled monolayer
SDS	Sodium dodecyl sulphate
SSC	Saline sodium citrate buffer
μTAS	Micro total-analysis system
TEM	Transmittance electron microscopy
Tris	Tris(hydroxylmethyl)aminomethane
UV	Ultraviolet

1: GENERAL INTRODUCTION

This chapter is a general introduction to compact discs (CDs) and literature research on CD technology for biomolecular detection and electroanalytical chemistry. It first provides the basics of optical compact discs including the composition and data structures, which are essential for the development of computer-readable disc-based bioassays (described later in the thesis). It is followed by descriptions of previous research carried out on CDs (in particular electroanalysis with CDtrodes[14-27] and disc-based microfluidics[28-32]).

1.1 From Biosensors to Point-of-Care Devices

1.1.1 Biosensors

Biosensors are devices that provide information on the identity and abundance of a certain biological analyte. There are three components to a biosensor: a biological sensing element, a transducing element, and displaying element. The biological sensing element consists of capture molecules, such as cell receptors, enzymes, antibodies, or nucleic acids, which recognize the analyte of interest. The transducing element then transforms this recognition event into a measurable signal that is correlated to the amount of analyte by means of optical, electrochemical, thermometric, piezoelectric, or magnetic readout.[1] The output should be presented in a form readable by the end user by the display unit.

Since the introduction of chip-based biosensors (microarrays) in the early 1990's, microarrays have significantly accelerated the generation of biological data.[2] With the same volume of biological sample, both multiplexation and miniaturization allow microarrays to gather a larger amount of data, thus saving time, labour, and reagents. DNA and protein microarrays are the two main streams of biochips. DNA chips allow molecular biologists to achieve gene expression profiling, providing them a global view of biological systems; they also allow genetic variations such as single nucleotide polymorphism and mutations to be revealed.[3,4] While being more difficult to handle than DNA molecules, proteins are the functional units of biological systems and are the targets of pharmaceutical intervention. This need motivated the advance of protein microarrays. In addition to measuring the abundance of proteins, the development of protein microarrays allows protein activities to be investigated.[4]

Immunoassays are powerful antibody-based biosensors utilizing the specific interactions between antigens and antibodies. In "indirect" immunoassays, specific antibodies are used to bind to immobilized antigens of interest. Labelled secondary antibodies are then allowed to interact with the bound primary antibodies. In another type of immunoassays, sandwich assays, the order of molecular binding is different. After immobilizing the antibodies of known specificity onto the substrate, the sample is introduced. The addition of specific detection antibodies that bind to the target protein in another epitope allows the detection to take place. This sandwich structure can increase the signal-to-noise ratio by reducing the background signal (non-specific interactions).

Without the capture antibody, all proteins in the sample can bind to the surface. In contrast, the immobilization of the capture antibody on the surface allows only the protein of interest to bind. Consequently, specificity and sensitivity of the method can be enhanced. Nonetheless, antibodies binding to two different epitopes of the same target protein are required. The detection antibodies are usually labelled with fluorescent dyes. When the detection antibodies are labelled with enzymes, this detection method is referred to as enzyme-linked immunosorbent assay or ELISA.[4] The enzyme changes the colour of a chromophore or cleaving a non-fluorescent substrate to a fluorescent product. Because the extent of colour change or the fluorescence intensity is related to the amount of binding event, the concentration of the analyte can be determined. Due to the enzymatic reaction, signal amplification can be achieved rapidly increasing the sensitivity of the test.[5]

1.1.2 Point-of-Care Devices

Current methods of diagnostics are usually time-consuming, labour-intensive, and often limited to biomedical laboratories or hospital settings due to their requirement for specialized and expensive equipment. To cope with limitations associated with current screening methods, point-of-care (POC) biosensors have been developed to allow the diagnosis to be done essentially anywhere. Point-of-care devices, by definition, refer to portable devices that give screening results in a short amount of time. Due to their portability, they can be used in a clinical laboratory, doctor's office, or at home at a lower cost. With these POC biosensors, we can obtain test results in less time; treatment

decisions can be made faster and post-treatment monitoring and disease recurrence surveillance can be improved, leading to better patient outcome.[1]

The glucose meter is a well-established POC device that is commercially available. It usually has a size of a palm and gives the test results within a few seconds. Its small size and fast response allow it to be accessible to the general public. Mass production has reduced its price significantly making it affordable. Patients can perform the test anywhere at anytime without the assistance of professionals.[6]

1.2 The Compact Disc System

1.2.1 CD structure

The disc is 120 mm in diameter and the centre hole is 15 mm in diameter which is for the player to hold the disc in place (Figure 1.1). The lead-in and lead-out areas start at radius 23 mm and 58 mm respectively; they notify the reader where the start and end of digital information are. The actual digital information starts at the radius 25 mm and extends to 58 mm at maximum.[7,8]

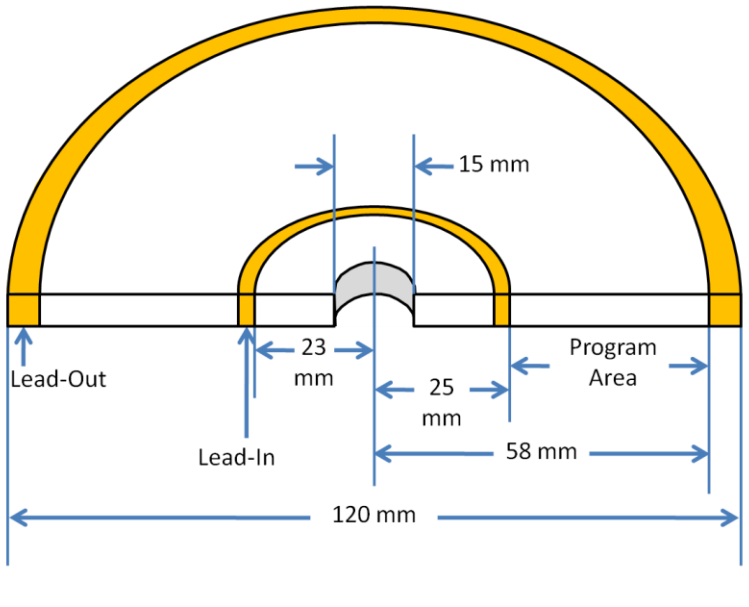

Figure 1.1. The specification of a disc.

There are several different types of CD's. The most basic CD format is the CD read-only-memory (CD-ROM). There are three layers in such a disc. The first layer from the bottom is a polycarbonate layer and has a thickness of 1.2 mm. There are pits embedded on the top surface of this layer for data storage (Figure 1.2a). The next layer up is a metallic layer that provides reflection when the CD is read by a laser. This layer is usually made of aluminum, silver, or gold and has a thickness of 50 to 100 nm. The top layer is a protective polymer layer that prevents the CD from scratches and it ranges from 10 to 30 μm; there is usually a 5-μm label that people print for identifying purposes.[8] In CD-recordables (CD-R's), there is an extra dye layer sandwiched between a reflective layer and a polycarbonate layer that has a spiral pre-groove structure embedded (Figure 1.2b). The ridge-groove structure on the polycarbonate layer guides the laser

beam during the processes of writing and reading. The dye layer of cyanine or phthalocyanine is spin coated onto the PC surface before the reflective metal is sputtered on the surface. According to the digital information to be written into the disc, the laser makes the dye layer transparent to expose the reflective layer by decomposing the dye.[9]

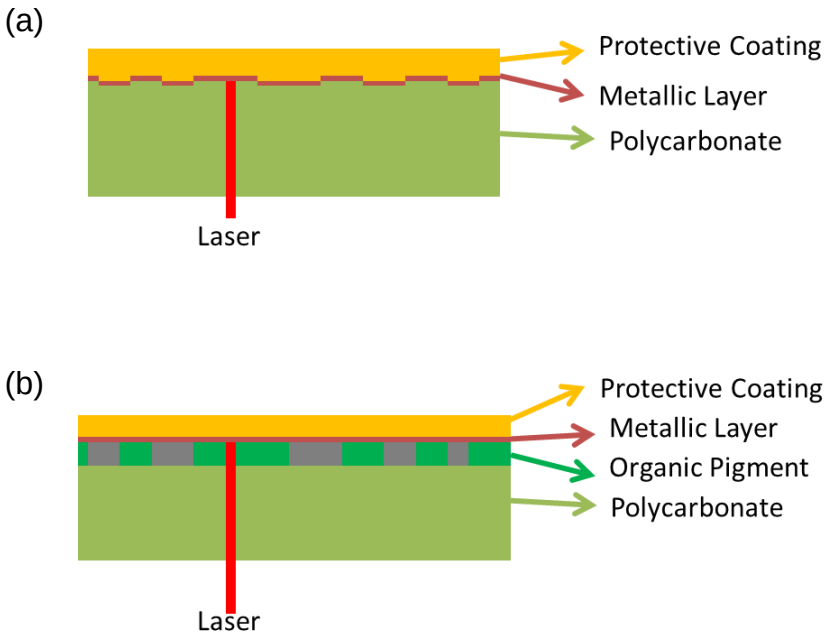

Figure 1.2. The layouts of a (a) CD-ROM and (b) CD-R.

1.2.2 Data Retrieval

To read the data stored in a CD, a laser of 780 nm is used. After emitted from a laser diode, the laser hits a semi-transparent mirror that rotates the plane of polarization of the light beams and directs the beams toward the disc surface (Figure 1.3). After making the divergent light rays parallel by a collimator, an objective lens focuses the laser on the disc's reflective pit surface. The reflected

light passes through the semi-transparent mirror that passes light in one plane but reflects light in the other plane, and strikes the photodiode. The outputs of the photodiode are then demodulated to yield the stored data.[10,11]

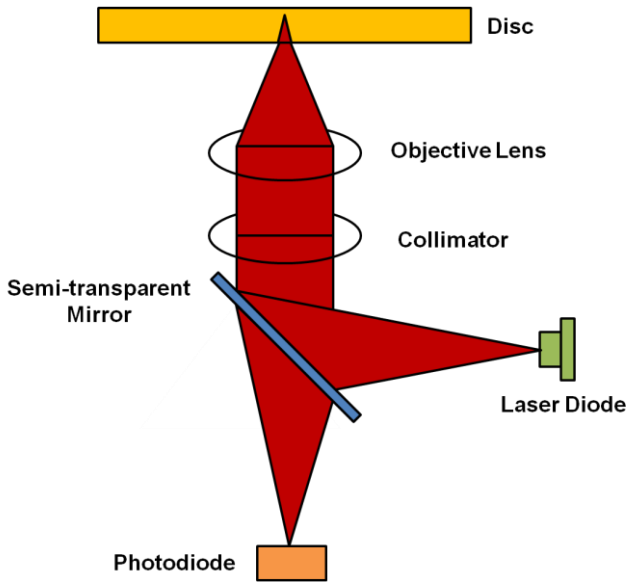

Figure 1.3. Compact disc laser pickup.

The spot size of this laser beam is 780 μm on the disc surface. Due to the refractive index of the polycarbonate, the thickness of the disc, and the numerical aperture of the laser's lens, the spot size of the laser beam is reduced to 1 μm at the pit surface. Because of the focusing, any object less than 0.5 mm becomes insignificant at the polycarbonate surface and produces no errors in the reading process.[8]

The laser of 780 nm passes through the polycarbonate layer and is focused on the region where the pits are. When the laser hits the pit, or land from

the laser's perspective, it is reflected back. Because of the change in refractive indices between air (N = 1) and polycarbonate (N = 1.55), the wavelength has decreased to approximately 500 nm for the duration of the laser inside the polycarbonate layer. Each pit is manufactured so that it is between 0.11 and 0.13 μm deep, which is approximately a quarter of the laser wavelength. When the laser travels from a pit to a land or vice versa, there is a difference of λ/2 in path lengths. This difference results in a destructive interference between the light reflected back from the land and that from the pit and leads to a reduction of intensity. These changes in intensity are then detected by a photodiode. When there is no change in path length either scanning through a land or a pit, a 0/1 is recorded. On the other hand, when there is a change in the reflected intensity (*i.e.* a transition from a land to a pit or vice versa), a 1/0 is recorded. This binary code is then converted to an electrical signal by a digital-audio converter, and thus information stored in a CD can be retrieved as music.[8]

1.2.3 Data Hierarchy

Each audio CD is read at a speed of 75 blocks per second. A block is composed of 98 frames, which are the smallest recognizable sections of data on a disc.[8] Each frame contains 3 bytes of synchronization, 1 byte of subcode, 24 bytes of audio data, and 8 bytes of parity.[12] The data structure of an audio CD is summarized in Figure 1.4. One byte of data is equivalent to 8 bits of binary data on the disc surface. Synchronization allows all the digital signals to be processed simultaneously. Subcode contains general information such as the start and end

of each track and table of contents. Parity is used for error detection and correction purposes, which will be discussed in more detail in the next section.[8,12]

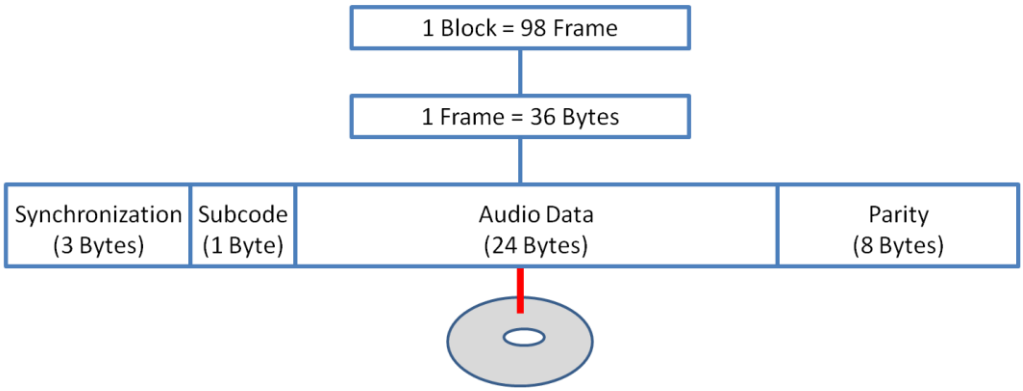

Figure 1.4. The data structure of an audio CD.

1.2.4 The Cross Interleave Reed-Solomon Code (CIRC)

There are two types of errors: random errors and burst errors. Random errors are errors randomly distributed in the data stream, usually introduced by manufacture imperfections in the polycarbonate substrate. Burst errors appear in large groups and are usually introduced by scratches or dust particles on the CD surface. To detect these errors, redundant data encoded in the disc are utilized.[13]

The CD system employs a sophisticated mechanism for error protection. This mechanism is known as the Cross Interleave Reed-Solomon code (CIRC). Data redundancy, in the form of repetitive data and parity bit, is the essence of error correction. Data are divided into groups and a parity bit is assigned to each group. A parity bit can only take two forms: odd or even. If the parity bit is set to

even (or odd), an odd (or even) parity bit would indicate an error. Using other data present, the correct value can be calculated. This is how random errors are corrected. To correct burst errors, interleaving is used. Interleaving is a process resembling shuffling a deck of cards. Data bytes in the data stream are rearranged in a way in which consecutive bytes are not adjacent to each other. Upon de-interleaving, the shuffled bytes are placed back to where they originally are. In this way, a burst error is fragmented into random errors that can be more easily corrected. This process is often repeated several times and is referred to as cross interleaving. In a CD player, a frame of 32 bytes is input to decoder C1, which corrects only one random error per frame (Figure 1.5). If no errors are detected, the frame of data will pass the decoder unprocessed. If there are more than one random errors or burst errors present, the entire frame will be flagged. The de-interleaver then places the bytes back to their original position. The C2 decoder is capable of correcting up to 4 bytes per frame. When more than 4 bytes are erroneous in a frame, the frame will be sent to the CD player's concealment circuit. New bytes will be generated based on adjacent valid data during a process known as interpolation. If interpolation is not possible, the audio output will be muted.[8]

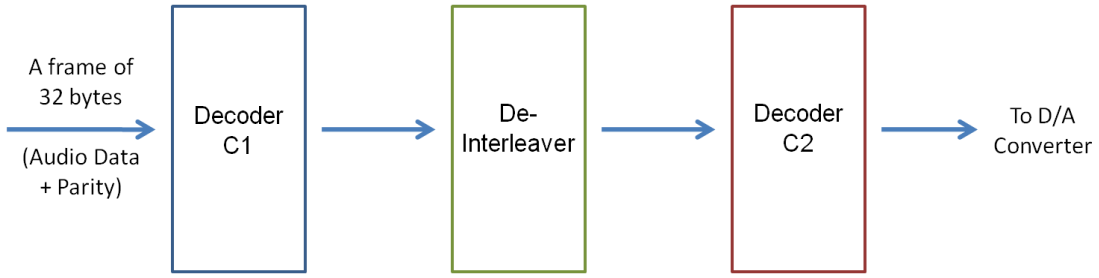

Figure 1.5. A simplified diagram of the CIRC decoding system.

1.3 Analytical Applications of Compact Discs

1.3.1 CDtrodes

The gold layer in the disc, which provides the reflective surface that reflects the laser to the photodiode, was of interest to many researchers because it is an inexpensive source of gold substrates for the electroanalytical research and the fabrication of self-assembled monolayers (SAM's).[14]

Self-assembly is one of the most profound interactions known in chemical and biological processes. This process has been utilized by chemists to produce a highly ordered monolayer on solid surfaces, and has a number of applications.[15] In nanofabrication, SAM's can be used to protect nanoparticles to avoid coalescence.[16] By using alkanethiolate SAM's on gold electrodes, kinetic study of long-range electron transfer is possible.[17-18] SAM's formed by using thiolated oligonucleotides on gold electrodes can be used in gene analysis and electrochemical DNA sensors formed in a similar manner is also available.[19-21]

The gold substrate from a regular CD can be easily prepared. After immersing the CD in concentrated HNO_3 for 3-5 min, the protective coating can

be peeled off. SAM's can then be formed on the CD by submersing the CD in the thiol solution of choice in absolute ethanol for 18-24 h (Figure 1.6).[14,15] The gold electrodes prepared from regular gold CD-R's using this method is given the name CDtrodes and can be used in electrochemical analyses. Angnes *et al*. have shown that the CDtrodes have comparable properties as commercial gold electrodes (Figure 1.7).[22] CDtrodes have then been used by many research groups for different applications. Copper[23] and mercury[24] were analyzed using electrochemical cells with gold CDtrodes. Organic analytes such as dipyrone were also analyzed using CDtrodes.[25] By constructing a spectroelectrochemical cell using CDtrodes, Daniel *et al*. allowed in situ UV-visible measurements and flow injection analysis to be done simultaneously. To do so, they used epoxy adhesive paste to fix two CDtrodes, which serve as the working and the auxiliary electrodes, on acrylic bases. A silicone rubber spacer was placed in between the two CDtrodes to provide a 200-μm space for the light beam to cross the cuvette (Figure 1.8).[26] Due to the popularity of miniaturization technologies, Daniel and his colleagues also constructed an array of gold electrodes on compact discs. An electrode pattern was designed and laser printed out onto wax paper. The toner on the wax paper was heat transferred onto the gold surface of a CD-R after the removal of the protective coating. Because the toner protects the gold layer from being etched in solution, the desired electrode pattern is thus created on the CD-R. The minimum size of the electrode arrays is limited by the resolution of the laser printer (about 100 μm). They also demonstrated the functionality and

reproducibility of these electrode arrays by using cyclic voltammetry and flow injection amperometric analysis.[27]

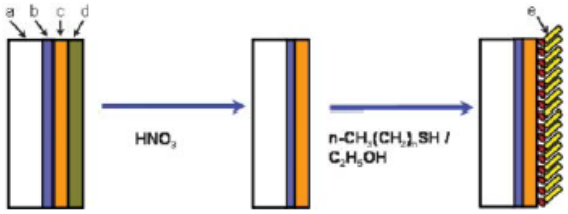

Figure 1.6. Self-assembly of alkanethiols onto gold substrates prepared from CD-R's, (a) polycarbonate base; (b) dye-photosensitive layer; (c) gold reflective layer; (d) protective polymer film; and (e) self-assembled monolayer (SAM).[14,15]

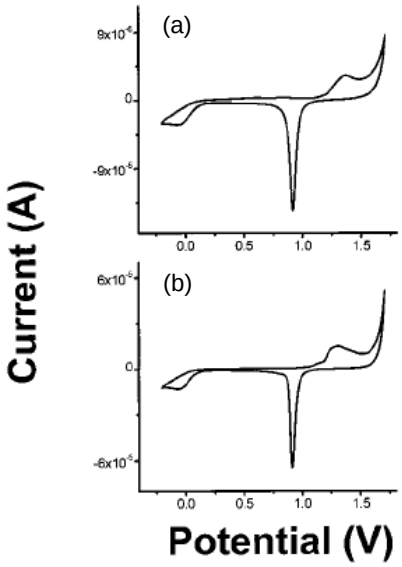

Figure 1.7. Comparative cyclic voltammograms with (a) commercial gold electrode (area, 3.15 mm^2) and (b) CDtrode (area, 2.83 mm^2) in 0.2 mol L^{-1} H_2SO_4; scan rate, 20 mV s^{-1}.[22]

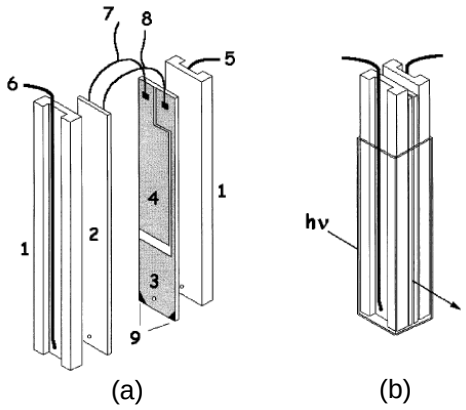

Figure 1.8. Schematic illustration of the spectroelectrochemical cell in (a) exploded view and (b) assembled into the cuvette. Components: 1) acrylic plate; 2) Au-CDtrode polycarbonate back plane; 3) Au-CDtrode working electrode area, 4) auxiliary electrode area; 5) solution inlet; 6) salt bridge to (not shown) reference electrode (Ag/AgCl); 7) electric interconnection of the twin auxiliary electrodes; 8) electric interconnection of the twin working electrodes; 9) silicone rubber spacer, 200 μm thick.[26]

1.3.2 Lab-on-a-CD

Since its introduction by Manz and coworkers in 1990, the concept of micro total-analysis systems (μTAS) has attracted many researchers' attention. Compared to the conventional approach to chemical analysis, μTAS, with its smaller size, offers many advantages such as portability, reduction of sample and reagent consumption, and high-throughput screening.[28]

Lab-on-a-CD is a device that integrates several laboratory functions on a CD-like platform. In addition to the advantages offered by μTAS, lab-on-a-CD systems require only a simple motor to provide the centrifugal forces needed for fluid manipulation. As the disc spins, centrifugal forces induced on sample fluids drive liquids radially outwards from the centre toward the edge of the disc.[29] As the liquid flow rate and microfluidic channel structure can be manipulated,

processes such as valving, decanting, calibration, mixing, metering, sample splitting, and separation can be performed on the disc with ease.[30] By embedding analytical measurements such as electrochemical, fluorescent, or absorption based detection methods on the same disc, test-specific information can be obtained. A typical setup of a lab-on-a-CD is shown in Figure 1.9.[30]

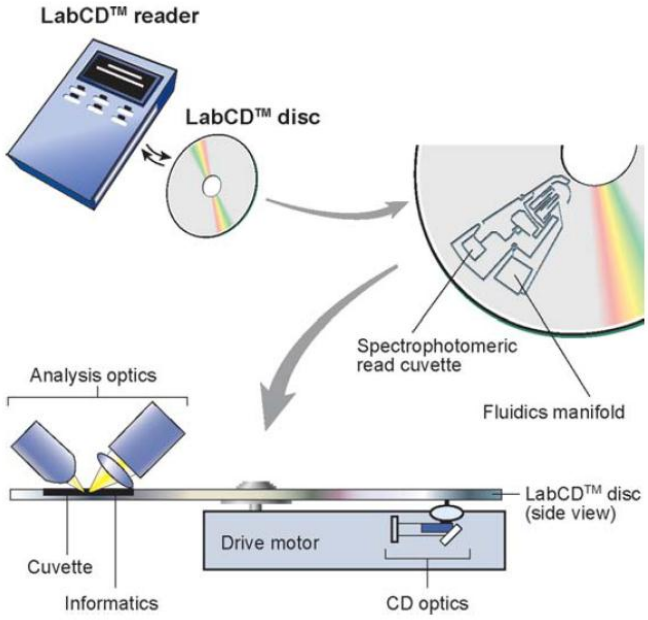

Figure 1.9. LabCD™ instrument and disposable disc. Here, the analytical result is obtained through reflection spectrophotometry.[30]

Applications such as PCR, immunoassays, and DNA microarray hybridization have been demonstrated on the microfluidic disk. By fixing a thermoelectric device for temperature control on the disk, Kellogg *et al*. allowed thermocycling to take place for the amplification of *E. coli* DNA. After this disk-based PCR step, they demonstrated the functionality of this PCR product by analyzing the DNA off-CD.[29] Lai *et al*. did enzyme-linked immunosorbent assay

(ELISA) for rat IgG on a CD-like microfluidic platform. By controlling centrifugal and capillary forces, the flow sequence of reagents and buffers in different chambers could be manipulated. The mixtures that reached the detection chamber were then analyzed with a fluorescence microscope (Figure 1.10). Even though the detection range of this method is similar to the conventional ELISA, this method has the advantage of consuming less reagent and requiring shorter assay time.[31] Peytavi and coworkers have performed DNA hybridization analysis on disks. They first designed a network of chambers and channels on polydimethylsiloxane (PDMS) and reversibly sealed the PDMS onto glass slides which had DNA capture probes immobilized to form a functional microfluidic unit. This unit was then mounted on a disk, which was fixed on a rotational device (Figure 1.11). The hybridization assay was done in 15 min and the hybridization signal was found to increase 10 folds as compared with the passive system.[32]

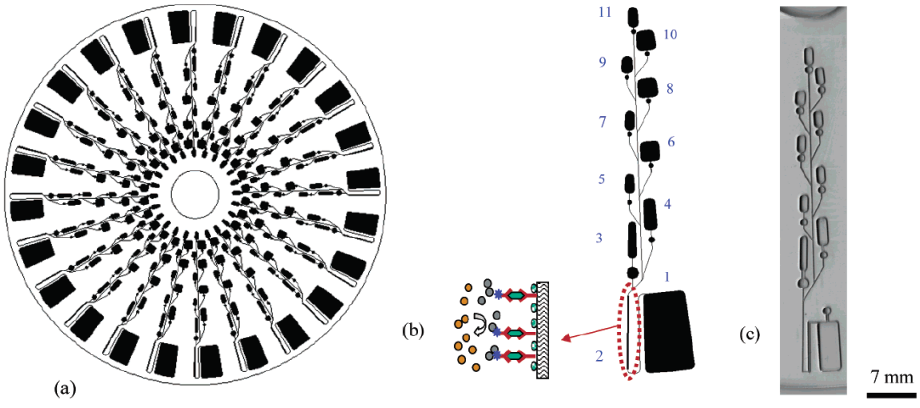

Figure 1.10. Schematics of (a) a CD-ELISA design with 24 sets of assays, (b) a single assay, (1, waste; 2, detection; 3, first antibody; 4, 6, 8, 10, washing; 5, blocking protein; 7, antigen/sample; 9, second antibody; and 11, substrate), and (c) photo of a single assay.[31]

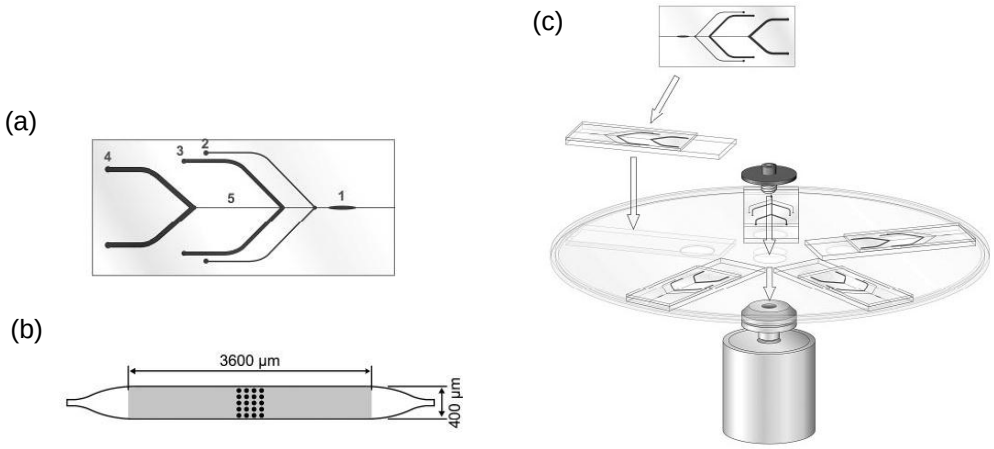

Figure 1.11. Schematic representation of the microfluidic system for microarray hybridization. (a), molded PDMS microfluidic unit juxtaposed on a glass slide consisting of chambers 2, 3, and 4, which allow the movement of reagents through a middle microchannel 5 to reach the hybridization chamber 1. (b), schematic view of the hybridization chamber of 400 X 3600 μm showing the area of the chamber that can accommodate up to 150 nucleic acid capture probes spotted onto a glass slide. (c), the microfluidic system molded in PDMS is applied to a glass slide on which the capture probes are arrayed. The glass slide is placed on a CD support that can hold up to 5 slides overlaid with PDMS. The hybridization reagents are positioned to be pumped sequentially through the hybridization chamber by centrifugal force starting with chamber 2.[32]

1.4 Objectives

The objective of this thesis is to explore the possibility of performing bioassays on unmodified CD's with standard computer drives. Rooted from the idea of POC devices, this thesis project introduces a versatile CD-based detection method, which aims to improve current ones to make molecular screenings more accessible to the general public, instead of being limited to the centralized laboratory and trained professionals. Another goal of the project is to lower the costs of molecular detections. The new technology utilizes the most popular consumer electronics (optical drive/CD player) to realize high-throughput

molecular screening, which will be suitable not only for qualitative determination, but also for quantitative analyses.

This thesis is divided into five chapters. After the first introductory chapter, chapters 2 to 4 describe the characterization of the CD, quantification of the molecular recognition reactions, and applications of this detection system, respectively. Chapter 5 presents the conclusion and suggests future directions for the project.

2: THE SURFACE CHEMISTRY TO PREPARE DISC-BASED BIOASSAYS*

The surface chemistry described in this chapter is essential to the fabrication of disc-based bioassays that are readable with conventional optical drives. In particular, a mild and efficient surface activation protocol has been developed to convert polycarbonate (PC) substrates, e.g., plastic bases of compact discs, to biochip platforms, and successfully tested by running DNA hybridization assays (DNA probe immobilization and target detection). In this protocol, UV/ozone treatment of PC sheets produces a hydrophilic surface with a high density of reactive carboxylic acid groups [$(4.8 \pm 0.2) \times 10^{-10}$ mol/cm^2] in less than 10 min at ambient conditions, and no significant aging or physical damage to the substrate is observed. Covalent immobilization of DNA probes via both passive (reagent-less photo-patterning and coupling in bulk solution phase) and flow-through (creation of microarrays with microfluidic channel plates) procedures has been demonstrated. Subsequent hybridization shows uniform and strong fluorescent signals for complementary target DNA and allows clear discrimination between fully complementary targets and strands with a single base-pair mismatch.

---

*Reproduced in part with permission from Li, Y.; Wang, Z.; Ou, L. M. L.; Yu, H.-Z. (2007) DNA Detection on Plastic: Surface Activation Protocol to Convert Polycarbonate Substrates to Biochip Platforms. *Anal. Chem.* 79: 426-433.

2.1 Introduction

Chip-based biosensors, notably DNA microarrays, have attracted increasing interest due to the many benefits of device miniaturization and parallel biomedical analysis. They are generally fabricated on glass, silicon or noble metal surfaces.[33-35] Synthetic polymers are promising alternative substrates because of their low specific gravity, high elasticity and low cost. In the past, nylon membranes have been used to make DNA microarrays. Their applications are limited as they exhibit lateral wicking characteristics, and the attached DNA probes tend to spread from the points of immobilization.[36] Other surface modification protocols that involve advanced organic synthesis and fabrication steps, such as using graft polymer coating on silicon or gold surfaces have been recently reported.[37-38]

Polycarbonate (PC) is an important thermoplastic because of its high optical clarity, tensile elongation and impact strength. It is the base material for the manufacture of compact discs (CDs) via an inexpensive injection molding protocol. Besides being popular information storage media, CDs have proven to be versatile tools/platforms for materials chemistry and biomedical research (as reviewed in Chapter 1).[14-32]

The activation of polymer surfaces is an important step in the process as it allows probes to attach to the surface. Without properly immobilizing probes onto the surface, the probes would be removed in the subsequent wash steps, which would render the later steps useless. In the past, the activation of polymer surfaces has relied primarily on high-power, prolonged ultraviolet (UV) irradiation.

Liu *et al*. irradiated PC with a UV lamp (4 W, 220 nm, 5 hours exposure) to improve the aqueous fluid transport in microchip capillary electrophoresis devices,[39] and to facilitate the DNA probe attachment to different plastic substrates (polystyrene (PS), PC, poly(methylmethacrylate) (PMMA) and polypropylene) in microfluidic channel arrays.[40] Welle and Gottwald studied the effects of UV irradiation (low pressure 15-W UV lamp, at 185 and 254 nm) of PS, PMMA and PC on cell adhesion *in vitro*.[41] McCarley and co-workers prepared polymer-based microanalytical devices by "mild" UV activation (15 mW/cm^2 at 254 nm) of PMMA and PC, and described their surface characteristics in detail.[42-44] Recently, Kimura reported a simple, direct immobilization method: UV- induced attachment of poly(dT)-modified DNA strands to PC, PMMA, and polyethylene terephthalate (PET).[45] These studies have demonstrated that UV light successfully converts PMMA to a bioreactive substrate with a high surface density of functional groups, leading to satisfactory results for DNA immobilization/hybridization.[39-46] In contrast, only limited success has been achieved for PC, mainly because of the low surface density of reactive groups,[42] auto-fluorescence,[40] and strong non-specific adsorption.[43] In the past, the UV/ozone protocol described herein has been primarily employed for removing hydrocarbons from metal and glass surfaces (e.g., cleaning of gold substrates for the preparation of high-quality alkanethiolate monolayers[47]), very little is known about its potential for surface activation of polymeric materials.[48] This chapter presents an efficient protocol for the activation of PC substrates (in particular, the plastic bases of CD's) and its potential application for the fabrication of

bioanalytical devices by direct immobilization of DNA probes via photo-patterning/coupling reactions[49] and by creating hybridization microarrays on microfluidic channel plates.[50-51]

2.2 Experimental Section

2.2.1 Surface Activation and Characterization

PC bases of CD's were provided by Millennium Compact Disc Industries Inc. (Vancouver, BC, Canada) or prepared from regular CD's (or CD-R's) by removing the reflective layer via scoring and vigorous rinsing with deionized water, removal of the dye layer with a rapid methanol rinse, a 10-min ultrasonication in 1:4 (v/v) methanol/water, and a final rinse with deionized water. The DNA oligomers (sequences are listed in Table 2.1) were of reversed-phase cartridge purification (RP1) grade and obtained from Sigma-Genosys (Oakville, ON, Canada).

The PC surface was "activated" in an UV/ozone system (model PSD-UV, Novascan Technologies, Inc.). This apparatus uses a low-pressure mercury lamp and generates UV emission at 185 (1.5 mW/cm^2) and 254 nm (15 mW/cm^2); the distance between the UV source and the PC sheets is 2.5 cm.

Water contact angle on activated PC surfaces were measured with an AST Optima system at ambient conditions (22-26°C, 43 ± 3% relative humidity) using a horizontal light beam to illuminate the liquid droplet. The contact angles measured here are the values of sessile liquid drops of either pure water or aqueous buffer solution. The surface topographies of the pristine and the

UV/ozone-treated PC surfaces were examined with an MFP-3D-SA AFM (Asylum Research Inc.) in tapping mode. Root-mean-square (rms) roughness factors were calculated using the IGOR Pro 4 software provided by the manufacturer.

To determine the surface density of carboxylic acid groups on activated PC surfaces, the UV/ozone-irradiated substrates were covered with a crystal violet solution (1 mM) for 5 min. After rinsing with water, the samples were incubated first with ethanol (80% v/v) and second with 0.10 M HCl (in 20% ethanol) until the dye could no longer be observed on the sample surface. Then the solutions from the two incubations were combined and absorbance readings were taken with a UV/Vis spectrometer.

2.2.2 Photo-Patterning and Passive DNA Immobilization/Hybridization

After the activation step, 10 μL of a 10 μM solution of DNA probe strands in 0.1 M MES (2-(N-morpholino)ethanesulfonic acid) buffer at pH 6.5 (also containing 5 mM EDC and 0.33 mM NHS) were spread onto the patterned PC surface (a TEM grid was placed on top during UV/ozone treatment), and the sample was incubated for 2 h under ambient conditions. For the hybridization test, a 10 μM solution (10 μL) of fluorescein-labeled DNA target strands (0.1 M $MgCl_2$ and 1 M NaCl in 10 mM Tris-HCl buffer) was spread onto the surface. DNA oligomers immobilized on the PC base of the CD (after hybridization) were imaged with a Zeiss LSM 410 confocal microscope (Oberkochen, Germany) equipped with krypton/argon laser sources.

2.2.3 Microfluidic DNA Microarrays on PC

The PDMS microchannel plates were prepared following the standard procedure reported in the literature.[52] The first channel plate (with 8-12 channels) was sealed with the activated PC for DNA probe immobilization. Probe DNA samples (typically 0.5 μL) were injected into the channel reservoirs on one side and passed through the channels by suction from the other ends. The solution was allowed to stay in the channel for 5 – 10 h at room temperature for DNA probe immobilization. To wash, Tris buffer was passed through the channels at least three times. Then the PDMS plate was peeled off, and the substrate was treated with glycogen solution to reduce (potential) nonspecific adsorption. Afterward, the second PDMS chip was placed on top of the substrate but in a perpendicular orientation. Hybridization was done by using Cy5-labeled DNA strands (0.1 – 2 μM); this step took place in a humid box at 20 – 40°C for 30 min. After hybridization, the PDMS plate was peeled off, and the PC chip was washed with buffers and dried with nitrogen. The chip was then scanned for specific hybridization using a confocal laser-fluorescence scanner (Typhoon 9410, Amersham Biosystems) at a resolution of 25 μm.

Radioisotope labelling measurements were performed by hybridizing a 50-pmol sample of 5'-modified ssDNA and 100 pmol of DNA template with a two-nucleotide-5' overhang (3'–TG–5') in 5 μL of buffer (50 mM Tris at pH 7.2, 10 mM $MgCl_2$, 0.1 mM DTT, 1 mg/mL BSA). It was heated at 90°C for 2 min, immediately followed by being cooled in an ice bath. The labelling reaction was started by adding 5 μL of the above buffer, containing 1 nmol of dATP, 6.67 pmol

of [α-^{32}P]dATP (3000 Ci/mmol, 10 mCi/mL), and 2 units of Klenow fragment of DNA polymerase I (Roch, Mannheim, Germany).[53] After 2 h, the labelled oligonucleotides were purified by precipitation with ethanol followed by 20% denaturing polyacrylamide gel electrophoresis. The procedure for immobilization and hybridization of ^{32}P-radiolabelled DNA on PC and the following washing procedure was the same as mentioned above. The DNA surface density was calculated by comparing the radioactivity of DNA immobilized on a certain area of the PC chip with that of a known amount of DNA. For this purpose, two control samples (known amount of ^{32}P-radiolabelled probe and target) were dropped on two reference PC chips, respectively, and allowed to air-dry without any washing. The radioactivity was read by phosphor imaging using the Typhoon 9410 scanner.

In the thermal and chemical stability tests, PC substrates with immobilized DNA probes were treated under PCR-like conditions (alternate immersions of the chip into three buffers at different temperatures) for up to 10 cycles. Each cycle consisted of a “denaturing step” at 90°C for 30 s, an “annealing step” at 50°C for 30 s, and an “extension step” at 72°C for 30 s.[45,54] After each cycle of the treatment, the slides was washed and used for hybridization experiments as described above.

2.3 Results and Discussion

2.3.1 Surface Activation and Characterization.

The PC base of a CD was activated by irradiation with low-power UV (1.5 mW/cm^2 at 185 nm, and 15 mW/cm^2 at 254 nm) and reaction with the ozone generated in the presence of ambient oxygen. The major advantage of this procedure over conventional high-power UV irradiation (without ozone) is its efficiency. As shown in Figure 2.1a, the water contact angle dropped from 88 ± 2° to 20 ± 2° after less than 10 min of UV/ozone treatment and remained constant thereafter. For comparison, this process takes more than 10 h when PC is irradiated with UV light at 254 nm in the absence of ozone (Figure 2.1b). The UV/ozone protocol is substantially more efficient than the UV-alone experiment reported recently,[42] in which a decrease of the water contact angle to 50° was achieved on PC after 2-h activation. The reaction durations reported in the literature to obtain hydrophilic PC surfaces vary significantly (from 60 min to more than 10 h), depending on the wavelength, power, and distance of the light source. Besides the observed rate acceleration, UV/ozone treatment also leads to a simple exponential decay (Figure 2.1a) of the surface wettability; in the absence of ozone, the contact angle decreases slowly at first and more rapidly later (Figure 2.1b).

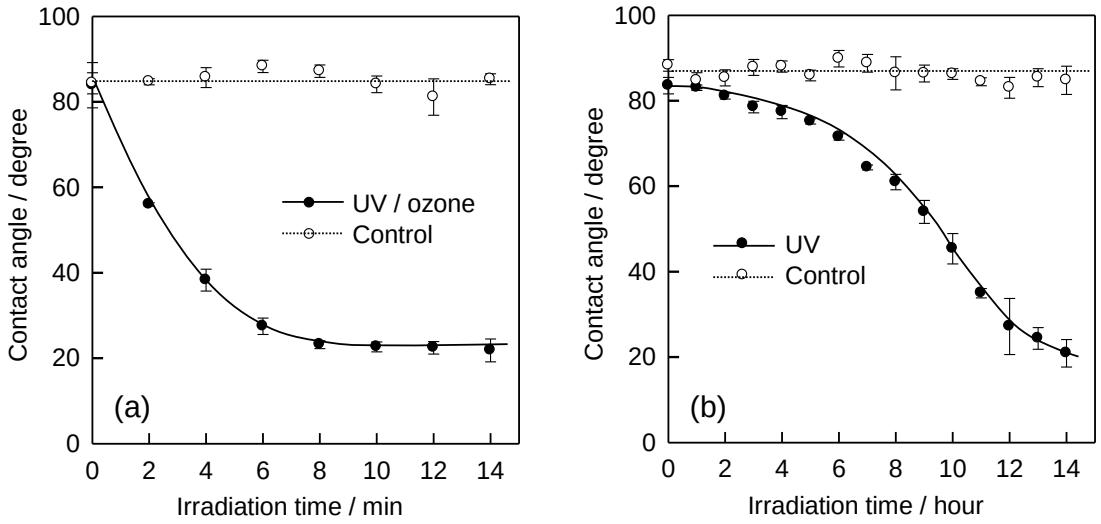

Figure 2.1. Dependence of water contact angle at the PC surface on activation time during (a) UV/ozone treatment and (b) conventional UV irradiation (λ = 254 nm). The dashed and solid lines are to direct the eyes only. Independent PC samples were treated for various periods of time under the specified conditions (UV/ozone or UV alone) and three data points were taken from each sample. After repeating the experiment four times, the overall averages and standard deviations were determined for constructing these curves shown in parts (a) and (b).

A major problem for potential applications upon surface activation is the so-called aging effect, i.e., the increase of hydrophobicity during sample storage. It is believed that reorganization of the polymer chains on the surface induces the hydrophilic groups to move into the bulk. As shown in Figure 2.2, the aging effects for PC surfaces treated with UV/ozone versus UV alone differ considerably in terms of time scales and final contact angles. With UV/ozone, the water contact angle increases initially and then remains constant at ~40°, which indicates that the surface remains reactive after several days while UV-treated samples show a gradual contact angle increase up to 60°. It is noted that the

angles measured on hydrophilic PC are widely scattered (Figure 2.2b), partially because below 40° the water droplets spread broadly across the surface.

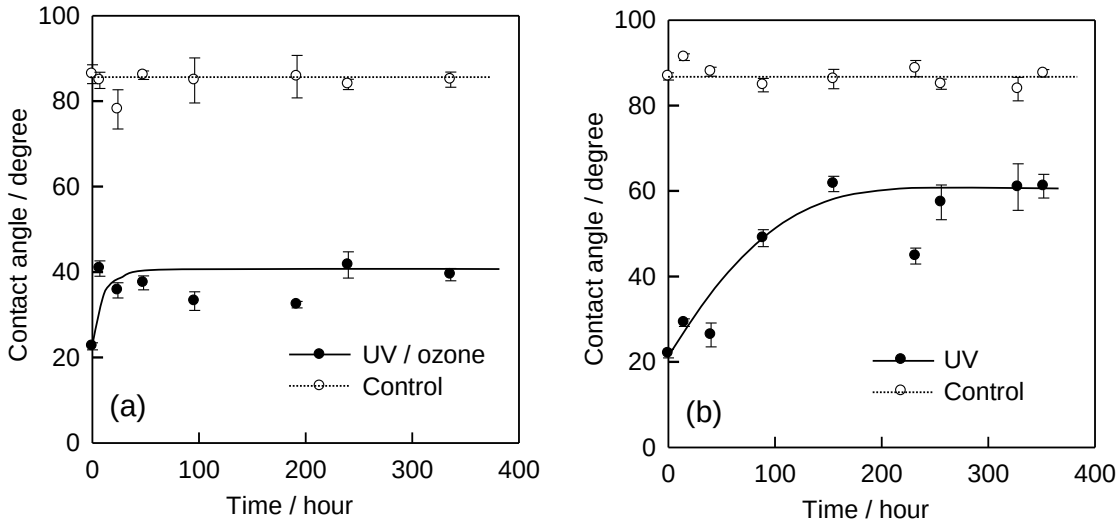

Figure 2.2. Dependence of water contact angle at the PC surface on storage time (aging) after initial activation by (a) 10-min UV/ozone treatment and (b) 15-h UV irradiation (λ = 254 nm). The dashed and solid lines are to direct the eyes only. Two independent samples were used for each of the UV/ozone and UV only irradiation conditions; three random regions were used for each data collection after the storage time specified. The data points and error bars shown in parts (a) and (b) are averages and standard deviations.

To confirm the formation of reactive COOH groups besides other polar functionalities (e.g. alcoholic OH) that also reduce the surface hydrophobicity, contact angle titrations were carried out. Figure 2.3 shows a typical titration curve (open circles): the contact angles of buffer solutions went through a smooth transition upon raising the pH from 4 to 9, due to the ionization of carboxylic acid groups.[55,56] The formation of carboxylate anions (COO^-) makes the surface more hydrophilic. In contrast, untreated surfaces (solid circles) display a constant angle over the entire pH range tested. It is remarkable that the difference between the

two “plateaus” is as high as 30°, indicating a high surface density of reactive COOH groups.[55] The pH range of the wettability switch is broader than that observed for caboxy-terminated alkyl monolayers on silicon,[57] which may be due to the generation of different types of carboxylic acids upon surface activation (e.g., R-COOH and R-CH_2COOH).[58,59] We note that phenolic OH groups can be generated on the PC surface upon UV/ozone treatment; however, the p*K*a values of phenols are much higher (8 – 10) than those of carboxylic acids. In addition, the presence of phenols will not interfere with the coupling chemistry for immobilization of DNA strands.

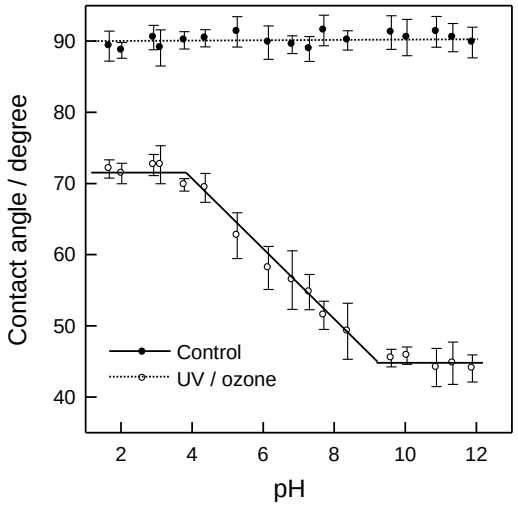

Figure 2.3. Contact angle titration curves of the untreated PC surface (solid circles) and of the PC surface treated with UV/ozone for 10 min (open circles). The dotted and solid lines are used to direct the eyes only. Four independent samples were prepared for constructing the titration curves. Three data points from each sample were obtained for each pH, and the error bars shown are the standard deviations.

To determine the surface density of carboxylic acid groups (-COOH) resulting from UV/ozone treatment, a cationic dye, crystal violet (Figure 2.4), was

added at a basic pH. This method relies on the electrostatic interactions between crystal violet molecules and carboxylate groups. The concentration of crystal violet released from the surface was calculated from Beer's law ($A = \varepsilon cl$) and used to determine the surface density of COOH groups. With an ε value of 100 $cm^2/\mu mol$, the calculated density is $(4.8 \pm 0.2) \times 10^{-10}$ mol/cm^2, which is an average over three samples. This value is significantly higher than that reported in the literature (~2.5×10^{-10} mol/cm^2, achieved by 1-h UV irradiation).[42]

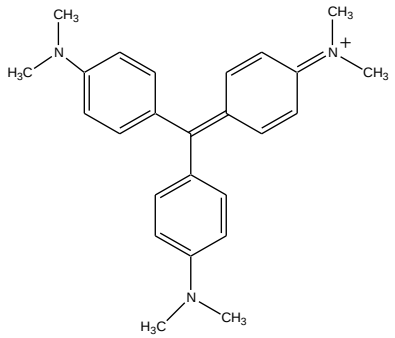

Figure 2.4. The structure of crystal violet.

To ensure the topography of the PC substrates (CD base) is not significantly altered upon UV/ozone treatment, the surfaces were examined by tapping-mode atomic force microscopy (AFM). Figure 2.5 shows the AFM images of (a) an untreated and (b) an activated PC surface. Both images reveal tracks of polishing on the mold caused by the injection molding procedure during CD manufacture. The surface roughness did not increase as indicated by the identical *z* scales (12 nm in both pictures) and similar rms roughness factors (2 – 3 nm). Instead, the UV/ozone-treated samples appear much smoother and less

porous; the rms roughness factor decreased from 3.0 ± 0.2 to 2.2 ± 0.2 nm. This indicates that the photo-oxidation and subsequent washing steps may remove some material from the surface that would be beneficial for the preparation of bioassays on PC substrates. The fact that the CDs were not physically damaged and remained readable guarantees the potential application of the UV/ozone activation protocol for the fabrication of biochip devices that are readable in standard optical drives (as described in Chapter 4).

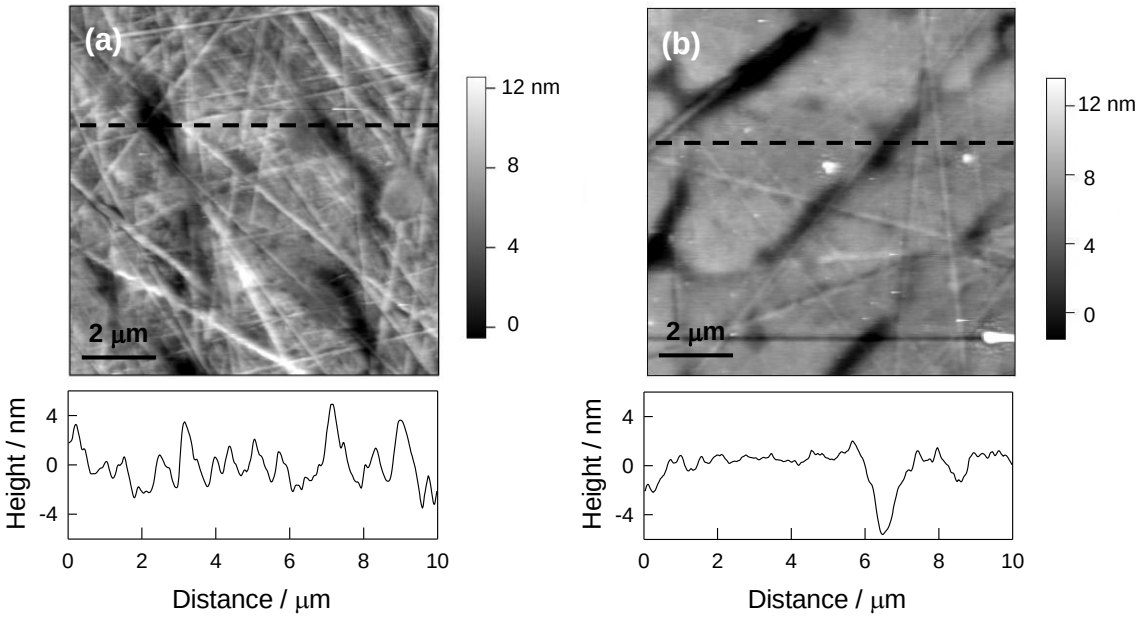

Figure 2.5. Representative AFM images and corresponding cross sections of the PC surfaces of a CD (a) before and (b) after UV/ozone treatment for 10 min.

The protocol described above is seemingly not much different from previous methods (UV irradiation without ozone);[39-46] however, it is substantially faster (short reaction time), more effective (the activated surface is more hydrophilic), and non-destructive (i.e., it does not physically damage the surface).

The photochemistry of PC under UV irradiation has been widely studied, and a two-stage reaction mechanism has been proposed to explain the generation of carboxylic acid groups.[46,58,59] At wavelengths between 254 and 300 nm, PC is known to undergo a photo-Fries reaction that results in the formation of phenyl salicylates and hydroxybenzophenones. The presence of atmospheric oxygen may induce the formation of an O_2-contact charge-transfer complex, which is the initial step in the photo-oxidation of aliphatic and aromatic alkenes. This complex may be converted to carboxylic acids via hydroperoxide intermediates. The presence of a moderate concentration of ozone (which decomposes at 254 nm) would certainly facilitate this process, thereby making the UV/ozone treatment a more efficient but less destructive surface activation protocol than prolonged UV irradiation, as proved experimentally for other polymeric materials (poly(dimethylsiloxane) (PDMS) in particular).[60-62] The detailed mechanism of PC activation by UV/ozone is not known at this stage, but its elucidation is beyond the scope of this thesis.

2.3.2 Photo-Patterning and Passive DNA Immobilization/Hybridization

Upon generation of reactive carboxylic acid groups, the CD surface is essentially converted into an effective platform for the construction of biochips. This potential application has been demonstrated first by the immobilization of DNA probe strands and subsequent hybridization with target samples with conventional incubation methods, i.e., by immersion of the activated PC substrates in bulk samples of modified DNA strands for coupling and hybridization.

Table 2.1. Oligonucleotide sequences of the probe and target DNA samples.

DNA Strand	Sequence
Probe I	5'-Amino-C6-CGC CGA TTG GAC AAA ACT TAA A-3'
Probe II	5'-Amino-C6-CGC CGA TTG GA***G*** AAA ACT TAA A-3'
Probe III	5'-Amino-C6-TTT AAG TTT TGT CCA ACT GGC G-3'
Target I	3'-GCG GCT AAC CTG TTT TGA ATT T-5'-fluorescein
Target II	3'-GCG GCT AAC CTG TTT TGA ATT T-5'-Cy5
Marker	5'-Amino-C6-CGC CGA TTG GAC AAA ACT TAA A-Cy5-3'

The PC base was first treated with UV/ozone for 10 min to generate carboxylic acid groups, using transmission electron microscopy (TEM) grids as photomasks to achieve surface activation and micropatterning in a single step.[42,49] To attach specific DNA probe strands (listed in Table 2.1) modified at their 5'-ends with amino groups via C6 linkers, amide linkages were formed via a 1-ethyl-3-(3'-dimethylaminopropyl)-carbodiimide (EDC) / N-hydroxysuccinimide (NHS) coupling reaction.[63] We note that the complementary probe sequence (Probe I) tested in this work has been previously used to detect plant pathogens (*Didymella bryoniae*).[64]

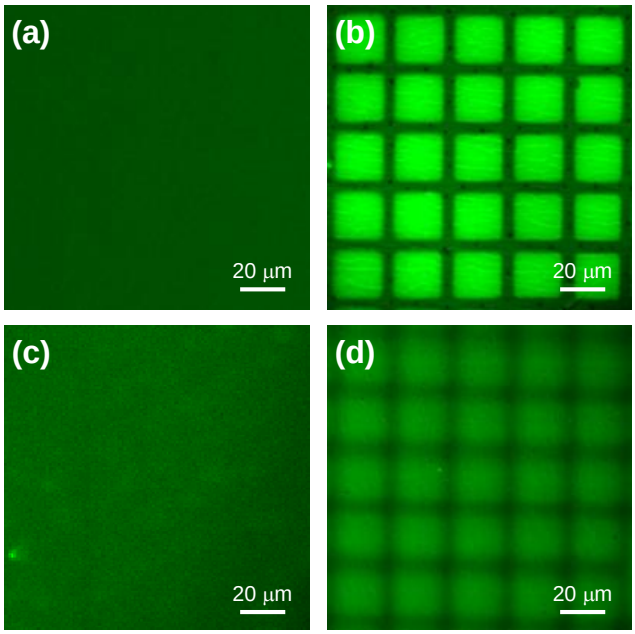

Figure 2.6. Typical fluorescence images of PC surfaces modified with DNA strands. (a) Before and (b) after hybridization of complementary DNA probe strands (probe I) with fluorescein-labeled DNA targets (target I); (c) probe and target DNA strands are noncomplementary (probe III); (d) single-base mismatch probe strands (probe II) after hybridization with fluorescein-labeled DNA targets.

In contrast to Figure 2.6a, upon hybridization of the immobilized complementary DNA probe strands (Probe I) with fluorescein-labeled DNA targets (Target I), distinct patterns were observed by fluorescence microscopy (Figure 2.6b). The areas exposed to UV/ozone fluoresced brightly, while unexposed areas (blocked by the TEM grid) did not produce significant signals (showing that no DNA strands were covalently immobilized at these locations). This also shows that non-specific adsorption of DNA target strands to the PC surface under passive adsorption conditions is negligible.

As controls, single-base mismatched and non-complementary amino-terminated DNA probes were tested by the same procedure. We found that the

hybridization of fluorescein-labeled target DNA with probe strands containing a single-base mismatch (Probe II) resulted in low-intensity fluorescence signals (Figure 2.6d). In comparison, no obvious patterns were discernible in the fluorescence images when the target and probe DNA strands (Probe III) were non-complementary (Figure 2.6c), demonstrating the high selectivity of the hybridization reactions on the activated PC surface. As shown in Figure 2.7, the relative fluorescence intensity of the single-base mismatch samples was less than 60% of that of the perfect match samples, and hybridization with non-complementary strands increased the fluorescence signal intensity only slightly (5%) relative to the background. It is true that the amide-coupling chemistry and the fluorescence detection of DNA hybridization are not original;[43] however, the sensitivity and selectivity we have achieved on UV/ozone-activated PC surfaces are unprecedented.

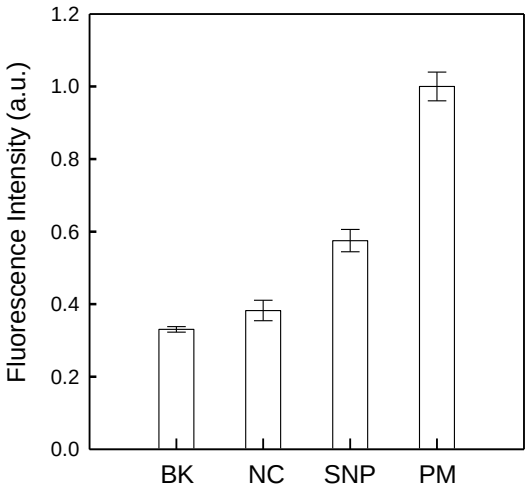

Figure 2.7. Relative fluorescence intensities of PC surfaces modified with DNA probe strands before (BK) and after hybridization of complementary DNA probe strands with fluorescein-labeled DNA targets (PM). NC, probe and target DNA strands are noncomplementary; SNP, single-base mismatch probe strands were used for hybridization. The intensity values and experimental uncertainties (error bars) were determined from three independent samples.

2.3.3 Microfluidic DNA Microarrays on PC

To demonstrate the potential applications of UV/ozone protocol for the activation of plastic materials in biochip fabrication, the creation of DNA microarrays on activated PC surfaces by a microfluidic method was then explored. This concept was initially reported by Biebuyck and co-workers in the late 1990s (patterned delivery of immunoglobulins);[50,51] it has been successfully employed by Corn's group to prepare ssDNA line arrays (1D) and DNA hybridization arrays (2D)[65] and by Situma *et al*. to generate DNA arrays (16 × 16) on photoactivated PMMA surfaces.[43] In comparison with traditional fabrication procedures (either on-chip photolithographic synthesis of DNA probes or robotic spotting of presynthesized oligonucleotides), the microfluidic method is simple

and does not require expensive facilities/instrumentation. As shown in Scheme 2.1, a PDMS plate is first put on the activated PC substrate (cut from a CD) for the immobilization of probe strands (to form a line array); after removal of this plate, the target samples are delivered with another PDMS plate. The hybridization event happens at the intersection of the microchannels on the second plate and the preformed probe line array. The oligonucleotide sequences for the probe and target DNA strands used in this experiment are also listed in Table 2.1.

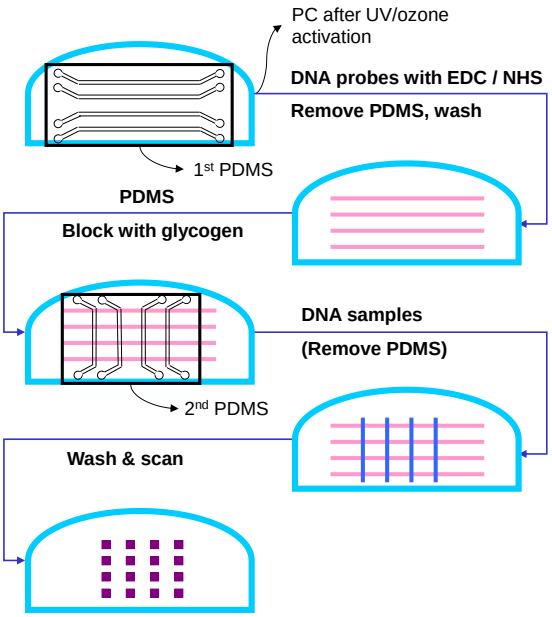

Scheme 2.1. A schematic presentation of the overall experimental procedure.

In order to examine the efficiency of flow-through immobilization of DNA probes on PC substrates, different concentrations of a marker strand modified with an amino group at the 5'-end for surface coupling and with a fluorescent tag (Cy5) at the 3'-end for imaging (Table 2.1) were used. As shown in Figure 2.8a, a

DNA line array is formed on the PC surface with a concentration as low as 0.5 μM (0.5 μL). The saturation surface density of marker strands is reached at a concentration of ~25 μM; higher concentrations will not lead to any higher contrast on the fluorescence image (Figure 2.8b). Consistently, the surface density of the immobilized marker strands determined by radioisotope labelling exhibited a trend similar to that of fluorescence measurements. When the concentration of marker solution reaches 25 μM, the surface density of the DNA strands will not increase further. The surface density of DNA probes was determined to be 5.4 ± 0.3 pmol/cm^2 via radioactivity measurements, which is smaller but of the same order of magnitude as the value reported for activated PMMA (10 pmol/cm^2).[54] It should be noted that, in this microfluidic format, the consumption of DNA sample is very little (~0.5 – 25 pmol). The rate of surface coupling may be limited by the diffusion of DNA molecules to the surface; this appears to be the primary reason for the more efficient immobilization in the flow-through setting. A larger amount of DNA molecules can be transported to the PC surface by convection (flow) than by passive incubation, as observed previously for the adsorption of thiolated DNA strands to gold surfaces through microchannels.[66] This interpretation is supported by the depletion effect, i.e., the apparent “fading” of the probe line at low marker concentrations (Figure 2.8a).

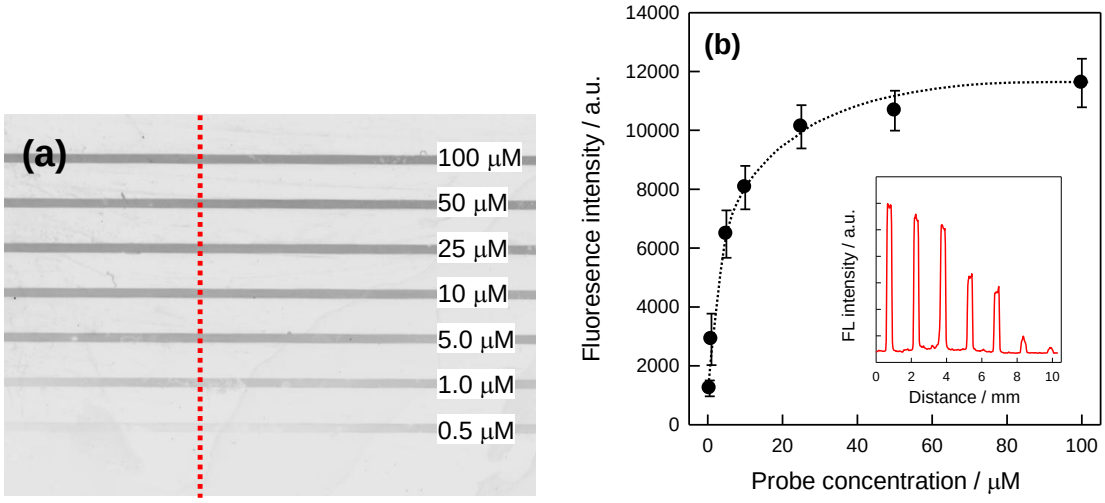

Figure 2.8. DNA probe line array prepared by delivering 0.5-μL samples of marker strands at different concentrations through microchannels on a PDMS plate. (a) Representative fluorescence image with the corresponding concentration labelled. (b) Relative fluorescence intensity as a function of the marker concentration. The experimental uncertainties shown as error bars were obtained by taking fluorescence intensities at three different regions of the same sample. The inset shows the line scan as marked in (a).

The efficient immobilization of ssDNA probes gave us the confidence to test the hybridization with specific DNA targets, assuming that nonspecific adsorption of DNA strands can be minimized. As shown in Figure 2.9, all hybridization sites (at the intersections) in two images have uniform shape and high fluorescence intensity, indicating the on-chip hybridization between complementary probe (Probe I) and target strands is efficient. However, the nonspecific adsorption of DNA strands on activated PC substrate is discernible, as illustrated by the “trails” left behind the target flow line in Figure 2.9a. This also indicates that not all the surface carboxylic acid groups have reacted with probe DNA strands. We have discovered that such nonspecific adsorption can be

effectively reduced by changing the hybridization buffer from Tris to SSC (with 0.15% SDS added). As shown in Figure 2.9b, SDS effectively blocks the nonspecific adsorption of DNA strands to the PC substrate, which has been applied to the hybridization experiments on glass substrates.[67] In this case, the hybridization sites are clearly distinct from the background (no discernible "trails" behind the target flow line) and exhibit overall uniformity (shape, size, and fluorescent intensity of each spot). In addition, the overall uniformity of hybridization spots can be easily repeated from one chip to another, demonstrating the reproducibility of the immobilization and hybridization experiments. The thermal and chemical stability of immobilized DNA probes on PC have been examined by varying the temperature (up to 90°C) and salt concentrations (up to 0.1 M), which did not result in significant changes (i.e., ~2% variation after each cycle) in their hybridization capabilities.

Besides the choice of buffer solution, the effect of target concentration on the hybridization results (the detection limit) was also systematically investigated. As shown in Figure 2.9c, the hybridization signal increases upon increasing the concentrations of target strand and reaches a maximum at 0.5 μM. This figure also shows that, even at the very low concentration of 0.1 μM (0.5 μL × 0.1 μM = 0.05 pmol), we can still observe a clear hybridization signal. The on-chip hybridization efficiency (the ratio of the amount of on-chip hybridized target to that of probe strands) determined by radioisotope labelling is ~5.6% (the target surface density is 0.30 ± 0.01 pmol/cm^2), which is close to the value (7.5%) reported on PMMA surfaces.[54]

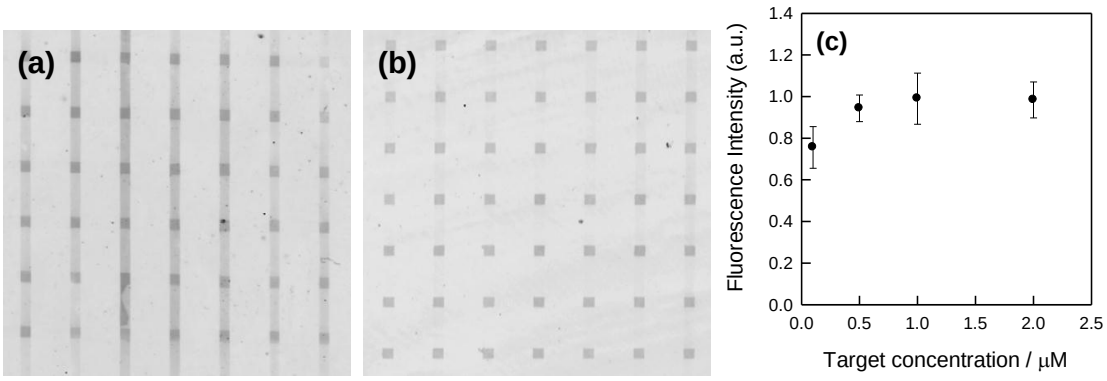

Figure 2.9. Fluorescence images of the hybridizations of complementary probe (Probe I) and target (1.0 μM) strands at 40°C for 30 min using different hybridization buffer solutions. (a) Tris buffer solution (pH 7.4, 10 mM Tris + 500 mM NaCl + 50 mM $MgCl_2$) and (b) 1 × SSC (pH 7.0, 150 mM NaCl + 15 mM sodium citrate) with 0.15% SDS added. (c) Relative intensity of fluorescence as a function of the target concentration (from 0.1 to 2.0 μM) under the conditions of (b). The experimental uncertainties in (c) were determined using the same way as specified in Figure 2.8.

Based on the effective probe immobilization and on-chip target hybridization, a DNA identification assay was performed to evaluate the hybridization of the same DNA target strand with three different probe strands that were immobilized with the first PDMS channel plate (Figure 2.10). Single-base mismatched (lines 1-3) and noncomplementary (line 4) amine-modified DNA probes were tested by the same procedure used for the complementary strands (lines 5–7). As shown in Figure 2.10a, the hybridization of Cy5-labelled target DNA with probe strands containing a single-base mismatch (Probe II) resulted in low-intensity fluorescence signals at the intersections with lines 1–3 (Figure 2.10b). In comparison, no signal was discernible in the fluorescence images when the target and probe DNA strands (Probe III) were noncomplementary (expected at the intersections with line 4), and the

fluorescence intensities at the intersections of target sample with lines 5–7 (complementary probe) were very high. We have also confirmed that the discrimination ratio is sensitive to assay conditions such as time and temperature. In addition, the hybridization spots were clearly distinct from the background (no “trails”), again confirming that nonspecific adsorption of DNA strands is not an issue here. Although the experimental conditions can be further optimized to achieve higher sensitivity, this result demonstrates the feasibility of creating DNA hybridization microarrays on PC substrates after UV/ozone activation and illustrates how the surface activation protocol can be applied to the preparation of bio-reactive substrates for the fabrication of microanalytical devices.

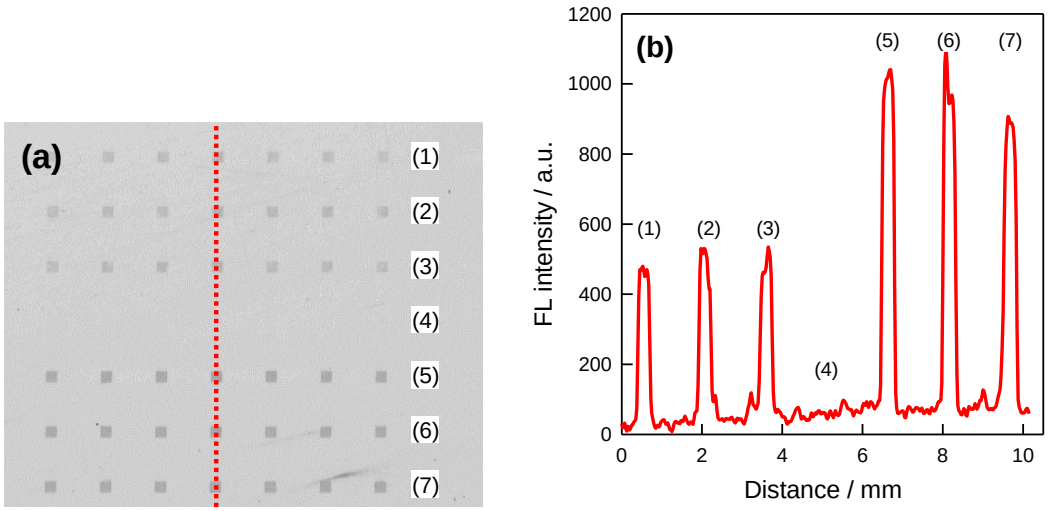

Figure 2.10. Hybridization experiments using microfluidic channels to deliver the same target sample (1 μM) on preformed DNA probe (50 μM) line array at 40°C for 5 min. (a) Fluorescence images with the probe numbers listed; (b) relative intensities of fluorescence vs. distance along the projection shown as dotted line in (a). Lines 5–7 were obtained with complementary probes (Probe I), line 4 with noncomplementary probes (Probe III), and lines 1–3 with strands containing a single base-pair mismatch (Probe II).

2.4 Conclusion

In summary, PC substrates (e.g., plastic bases of CDs) can be readily converted to a novel polymeric platform for the fabrication of chip-based biosensing devices (DNA microarray as an example) by brief UV/ozone treatment. The method is rapid (less than 10 min), efficient (yielding a high surface density of COOH), and nondestructive (surface morphology is not altered). The fabrication procedure (activation, patterning, and coupling) is simple and effective, and hybridization is highly sensitive and selective. Both passive and flow-through immobilization/hybridization experiments with various DNA probe-target complements have successfully detected single base-pair mismatches and reduced nonspecific adsorption. The surface chemistry described herein may find applications well outside the DNA microarray area: it is not overemphasized that the value of this method extends far beyond the simple examples presented in this paper; i.e., it is potentially useful for the development of disposable plastic biochips and the fabrication of biomedical devices that are readable with conventional CD drives.

3: READING DISC-BASED BIOASSAYS WITH STANDARD OPTICAL DRIVES*

A digital signal readout protocol for screening disc-based bioassays with standard optical drives of ordinary desktop/notebook computers is described in this chapter. A biochemical recognition reaction, i.e. biotin-streptavidin binding, was performed directly on a compact disc in a line array format with the help of microfluidic channel plates. Being well-correlated with the optical darkness of the binding sites (after signal enhancement by gold nanoparticle-promoted autometallography), the reading error levels of prerecorded audio files can serve as a quantitative measure of biochemical interaction. Because no modification to either hardware or software is needed, it promises a platform technology for rapid, low-cost, and high-throughput point-of-care biomedical diagnostics.

3.1 Introduction

As mentioned previously, microarray technology is a powerful tool for the high-throughput analysis of specific interactions between biological macromolecules (DNA, proteins, and carbohydrates). However, its applications (e.g., gene profiling, clinical diagnosis, immunoassays, and drug discovery) are currently limited to well-funded biomedical laboratories or hospital settings due to the requirement for expensive equipment (such as robotic spotters and laser fluorescence scanners).[68-71] Therefore, the development of inexpensive materials and tools for rapid biomolecular screening is important to the improvement of public health care, particularly for early-stage, on-site biomedical diagnostics. Compact disc (CD) technology is a promising candidate,[4,14] as it may offer versatile fabrication materials and convenient optical reading devices for microarray biochips. It has been shown in Chapter 2 that polycarbonate (PC) plates can be employed as alternative substrates to glass slides/silicon wafers for the preparation of DNA hybridization assays.[42,72,73] In addition, the characteristic optical phenomena occurring on the metal layer of a CD can be utilized to develop biosensors based on interferometry[74] or surface plasmon resonance.[75] If microfluidic functions are integrated with CDs, particularly the control of fluid transfer by disc spinning, laboratory-on-a-disc devices can be fabricated,[30,76] which have already attracted widespread interest in commerce (as reviewed in Chapter 1).[28-32]

Recent research to adapt computer drives as optical readout devices for biochips has been focused on innovative hardware modifications. With a second

laser-based detector attached on the upper part of a commercial CD drive, Alexandre *et al*. fabricated a double-sided reader to examine both numeric and genomic information on "bioCDs".[77] Barathur *et al*. reported that a modified optical drive can be used to read special discs with embedded microfluidic channels.[78] Recently, Lange *et al*. converted the pickup unit inside a CD drive to a laser scanning microscope to monitor the light reflection from gold nanoparticle-stained immunoassays microcontact-printed on CD surfaces.[79] Potyrailo *et al*. were able to acquire analog signals directly from the photodiode of a DVD/CD drive for the quantification of metal cations adsorbed on the disc surface.[80] Maquieira and co-workers detected DNA hybridization spots and immunoassays located on the top side of the CD by installing an additional photodiode to monitor the light transmitted through the disc.[81,82]

Meanwhile, other scientists have explored software approaches to analyze the digital signals obtained from a CD. The protocol pioneered by La Clair *et al*. for screening ligand-protein interactions on CDs was based on an error determination routine, for which a specially designed software was used to create unique data structures and to detect the reading errors by comparing the original with the retrieved data byte by byte.[83,84] Nevertheless, the multistep phosphorylation reactions for attaching ligand molecules to the polycarbonate surface reported therein need to be carefully handled,[83] as polycarbonate is not compatible with harsh organic solvents (e.g., prolonged exposure to acetonitrile or acetone will ruin the optical properties of CD substrates).[85] The detection sensitivity may also be limited because unlabeled biomolecules (usually smaller

than 10 nm) are not large enough to either effectively block/diffract the laser beam (780 nm) in a typical CD player[4,79] or to create significant interferometric signals.[74] Jones employed CD drives as photonic signal processing devices (optical microscopes) to image stained bacterial cells physically adsorbed on disc;[86] with the typical size of a cell ranging from a few to tens of micrometers, this is sufficient to disrupt the laser reading process. Since the entire CD was used for one type of stained cells in his experiments,[86] the potential of high-throughput analysis and the detection of biorecognition reactions at the molecular level deserves further investigations.

This chapter describes a novel readout protocol, which takes advantage of the reading-error correction function embedded in standard audio CDs, for the multiplex screening of biomolecular binding events. After “enhancement” of the assay signals by autometallography,[87-89] a free CD-quality analysis program is employed to detect and quantify the binding events. Because this technique does not require any changes to the computer hardware or software, it is readily accessible and suitable as platform technology for rapid, high-throughput, and point-of-care biomedical diagnostics. In addition, the surface chemistry we have demonstrated herein, i.e., to prepare robust, multiplex bioassays (for biotin-streptavidin binding interaction) on polycarbonate surfaces via covalent bonding, is potentially useful in the fabrication of other types of polymer-based microanalytical devices.[42,72,73]

3.2 Experimental Section

3.2.1 Surface Reactions and Characterization on CD-Rs

After recording, the PC surface was cleaned with ethanol and then activated in a UV/ozone cleaner (model PSD-UV, Novascan Technologies, Inc.) for 15 min. The disc was subsequently immersed in a 0.1 M phosphate buffer at pH 6.0 (also containing 5 mM 1-ethyl-3-(3′-dimethylaminopropyl)-carbodiimide and 0.33 mM *N*-hydroxysuccinimide (NHS)) for 5 h. After the NHS activation step, 10 μL of a 30 μM solution of amine-PEO_3-biotin (biotinyl-3,6,9-trioxaundecanediamine, Pierce Biotechnology Inc.) in 0.1 M phosphate buffer at pH 7.0 was delivered onto the PC surface through a mask (made from a PDMS plate), and the disc was kept in a humid box (a sealed plastic container with its bottom filled with water) for 5 h. After the PDMS mask was peeled off, the reaction zone was passivated by treatment with a 20 mM phosphate blocking buffer at pH 7.4 (containing 150 mM NaCl, 0.8% bovine serum albumin (BSA), 0.1% gelatin, 0.05% Tween 20, and 0.05% NaN_3) for 15 min to reduce nonspecific adsorption. Then a second PDMS plate with six microchannels oriented perpendicularly was placed on top of the disc. Five different concentrations of gold-conjugated streptavidin (1.4-nm diameter, Nanoprobes Inc.) solutions (0.1, 0.2, 0.4, 0.8, and 1.6 μg/mL) in 20 mM phosphate buffer (pH 7.4, 150 mM NaCl, 0.1% BSA, and 0.05% NaN_3) were injected into the channel reservoirs on one side and passed through the channels by suction from the other ends. The solutions were allowed to stay in the channels for 60 min at room temperature. After the PDMS plate was peeled off, the chip was washed with the

buffer, dried under N_2, and subjected to the silver staining treatment. Before the silver staining treatment, the biomolecule-modified CD-Rs were thoroughly washed with distilled water to remove anions (especially chloride). After washing, they were immersed in a freshly made silver enhancement solution for different periods of time. A reagent kit for silver enhancement reaction (LI Silver, Nanoprobes Inc.), which consists of two solutions, silver salt (silver acetate) and reducing agent (hydroquinone) respectively, was used as directed.

Optical images of all samples (the binding strips formed on CDs) were captured by a Motic Digital Microscope (DM143, Micro-Optic Industrial Group Co.) and analyzed by measurement of position and size (area) of each binding strip upon silver enhancement. The ODR of each strip was determined by measuring its average intensity (I_s), using the luminosity histogram tool of a Photoshop software, and compared to the value for the background (I_b).[89]

The surface topographies of the binding assays were examined with an MFP-3D-SA atomic force microscope (Asylum Research, Inc.) in tapping mode using a rotated monolithic silicon tip (Innovative Solutions Bulgaria Ltd., resonance frequency 13 kHz, force constant 0.2 N/m). The number, size, and morphology of the particles after silver enhancement were analyzed with IGOR Pro 4 software.

3.2.2 Digital Readout Protocols

3.2.2.1 Reading Error Numbers per Frame

Before reaction, audio information (such as WAV files) was burned into a blank CD-R (Mitsui Inc.). Three different systems (drive plus corresponding software), PX-755UF CD/DVD writer (Plextor Corp.) + PlexTools Professional (LE V3.12, downloaded from http://www.plextools.com), Plextor PX-760A CD/DVD writer (Plextor Corp.) + PlexTools Professional, and SHW-160P6S CD/DVD writer (Liteon It Corp., OEM)+ Kprobe (V2.50, downloaded from http://www.k-probe.com), were tested for biomolecular screening. The free Plextor Professional program runs on PC-Windows; it was used in this work to generate the error plots presented in Results. For error tests, this program controls the CD drive to run at an 8× speed, so that it typically takes 10 min to screen the entire CD and less than 2 min to screen a specified zone. After reading, it will export an error distribution plot and provide a statistical result on error numbers and types.

3.2.2.2 Reading Erroneous Bits

Audio data was recorded on RiDATA Silver-Silver 700 MB CD-Rs with Nero 7 (Ultra Edition). A single audio file of 5MB size repeated 60 times was written on each of two CDs for a set of experiments, one for the detection and the other as a reference to compare the hexadecimal data of the erroneous sectors with clean sectors. In each case, at least five different concentrations of streptavidin-gold nanoconjugate were tested.

IsoBuster was used as the software to detect and quantitate the bioassays on CDs. This is a data recovery tool compatible with multi-file systems, multi-hard media (CD/DVD/BD/HD DVD), and multi-soft media (various CD and DVD data formats), which provides the freedom to use any data format/media to conduct biomolecule detection. Though other CD scanning softwares have the ability to acquire the block error rate from media, they only count error frames, but not to the byte-by-byte details (as can be done with the single sector extraction utility of IsoBuster). It performs surface scans on hard media to check for physical reading errors which are identified and saved as a list of erroneous files. This utility is further exploited by the single sector extraction function which enables viewing of the exact sector and its erroneous data. The sector viewer gives the comprehensive logical block address to pinpoint the erroneous sector to the resolution of individual bits. This feature displays the hexadecimal data of a particular sector, allowing a comparison of the erroneous data with reference data.

3.3 Results and Discussion

3.3.1 Probe Immobilization and Signal Amplification

The UV/ozone surface treatment/amide coupling protocol and the gold nanoparticle-based autometallography method were integrated to accomplish the immobilization of probe molecules and signal enhancement. Figure 3.1a illustrates the surface reaction procedures for a typical assay. The PC face of a CD/CD-R was first irradiated with UV light in the presence of ozone to produce a hydrophilic surface with a high density of carboxylic acid groups (step 1). Then

the probe molecules, biotin, were covalently attached to the PC surface via amide coupling (step 2). By using microfluidic channel plates made of poly(dimethylsiloxane) (PDMS) as on-disc sample delivery and positioning tools,[43,73] the immobilization and binding reactions can be carried out in a flexible arraying format and at any desired location. The biochemical binding reactions on the disc surface were monitored initially with the conventional fluorescence (FL) method. The binding assays for fluorescence detection were prepared on transparent PC plates made from CD-Rs by removal of the metal and dye layers. Instead of gold-conjugated streptavidin, Cy3-modified streptavidin was used. The assays were then scanned with a confocal laser-fluorescence scanner at a resolution of 25 μm. Figure 3.2 shows the data for the binding assay for biotin/streptavidin. The results confirmed that the immobilization of the probes on the PC surface and the subsequent recognition of target molecules are efficient and sensitive. The detection limit and dynamic range were found to be 1.25 μg/mL and 1.25 – 10 μg/mL respectively for the binding assay. It should be noted that the surface activation procedure for PC substrate also works well for the attachment of small ligands and proteins.

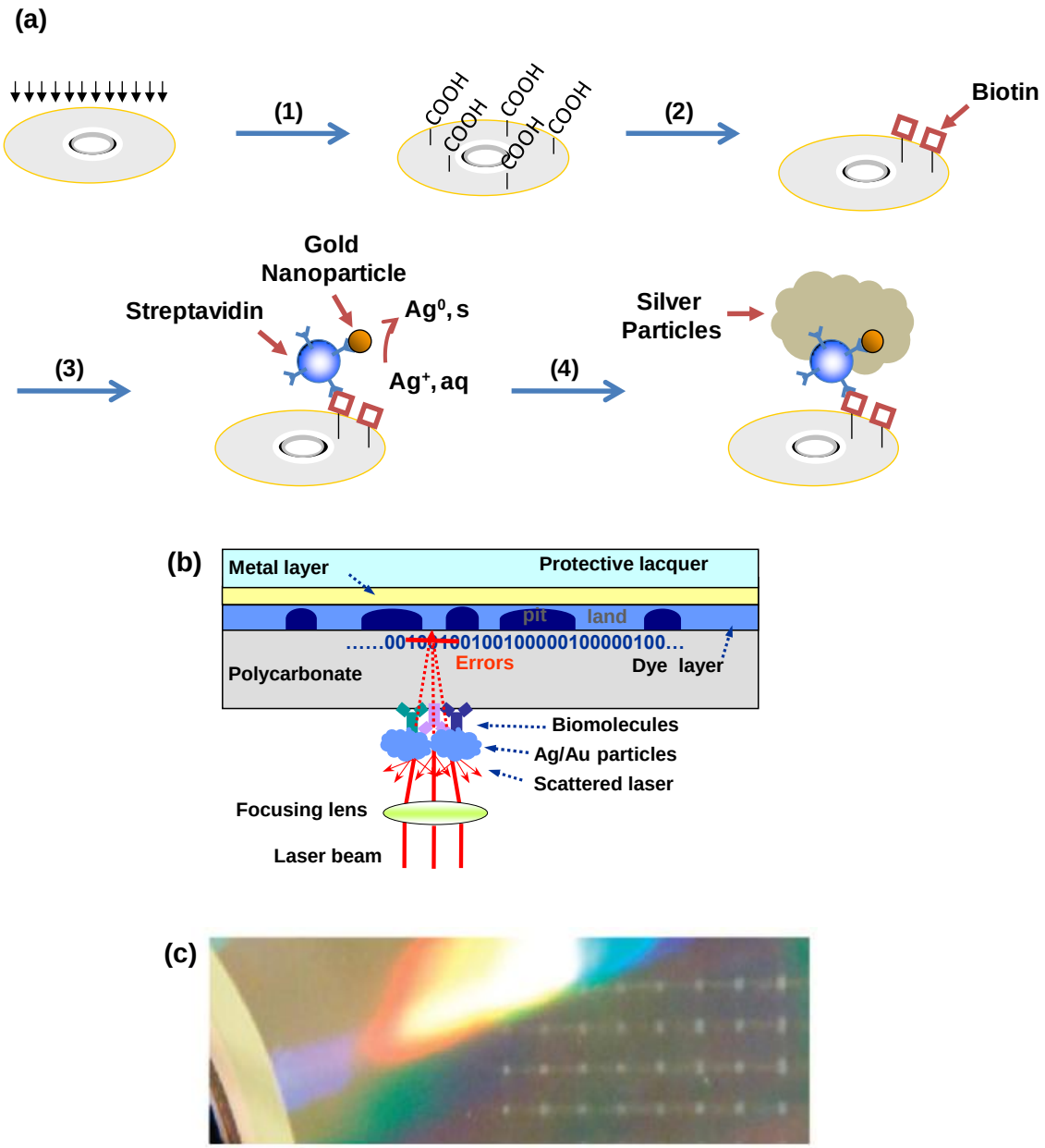

Figure 3.1. (a) Preparation of disc-based bioassay and signal amplification via gold/silver staining. (1) UV/ozone activation to generate carboxylic acid groups on CD; (2) immobilization of amino-tethered biotin probe strands via amide coupling; (3) binding of gold nanoparticle-streptavidin conjugates; (4) reductive precipitation of silver particles for signal enhancement. (b) Digital reading of bioassay with CD drive: the biomolecule/nanoparticle conjugates block the reading laser and generate significant errors. (c) An optical image of the microarray formed on a regular CD-R according to the above surface reaction and signal amplification procedure.

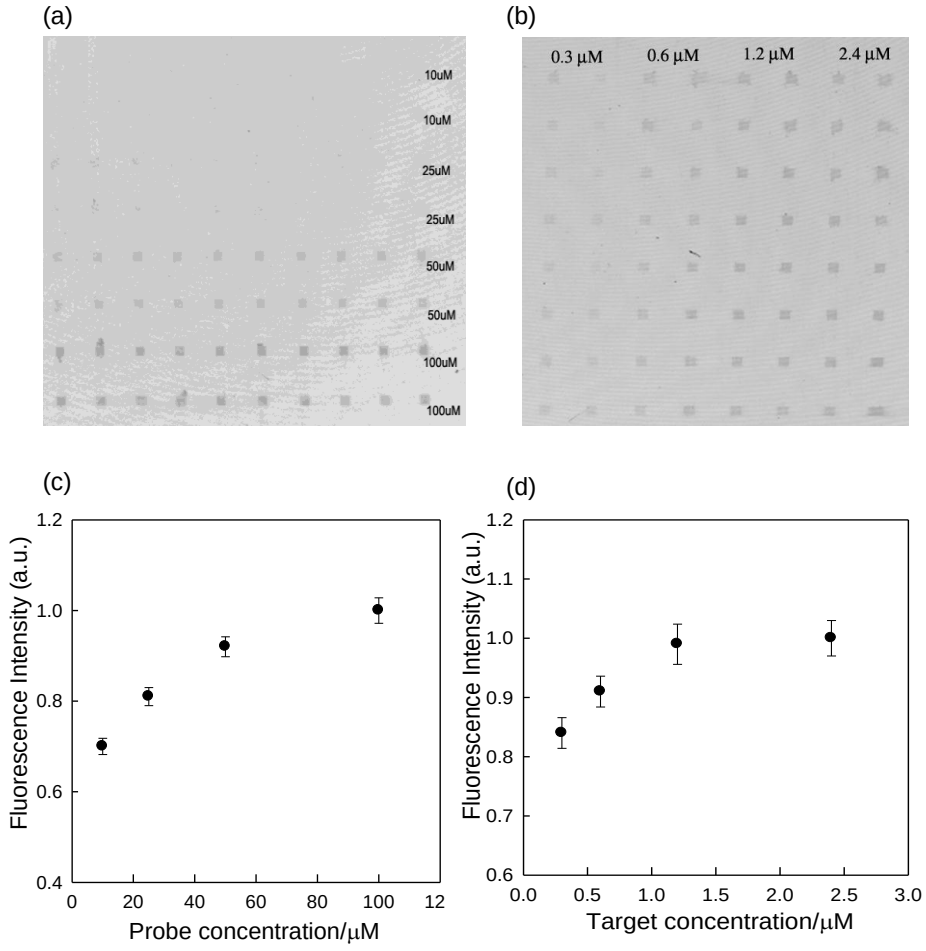

Figure 3.2. Representative fluorescence images of biotin-streptavidin binding assays on disc at different concentrations of biotin (a) or streptavidin (b). Relative fluorescence intensity as a function of probe (c) or target concentration (d). The experimental uncertainties shown as error bars in (c) and (d) were obtained by measuring the fluorescence intensities at three different regions of the same sample.

Objects of larger than 500 μm size are needed to induce significant disruption of the laser light reflection (to create "readable" signals) of a standard optical drive.[8] Since most biological macromolecules are too small to be detected by the reading system of a standard computer drive, we amplified the binding signals by autometallography.[87-89] Steps 3 and 4 of Figure 3.1a illustrate the

procedure for the biotin/streptavidin assay. Immobilized biotin was treated with gold nanoparticle-streptavidin conjugate (step 3). Silver was then deposited on the gold "seed" (step 5) to increase the particle size from a few to several hundreds of nanometers. As shown in Figure 3.1b, the large silver particles would block the laser beam hitting them and cause significant scattering,[79] thereby producing reading errors detectable by the optical drive. In fact, at saturated concentrations, the binding sites could even be observed with the naked eye or with a standard flatbed scanner (Figure 3.1c).

3.3.2 Digital Readout Protocols

3.3.2.1 Reading Error Numbers per Frame

This bioassay screening protocol is based on the analysis of reading errors produced on pre-recorded audio files by molecular binding events; i.e., the position and level of the resulting reading error correspond to the physical location and the intensity of the bioassay signal, respectively. In fact, every optical drive is "smart" enough to distinguish and correct the errors occurring in the reading process. To do this, it employs an algorithm called Cross Interleave Reed-Solomon Code (CIRC).[13] This coding system uses a data-interleaving strategy to record and distribute the original data (including potential errors) and employs a parity checking function (redundant data) to protect them.[8,13] Upon playing, the CD drive only needs to decode the data in a reverse sequence and extract the parity bits (redundant data) to check their accuracy. Any disagreement during the parity check indicates an error. Upon playback, after demodulation of each frame, each base unit (including 24 bytes of audio and 8

bytes of parity checking data) of the audio file is sent to the CIRC decoder for deinterleaving, error detection, and correction. Because every block of audio data passing through the CIRC decoder has an address corresponding to a specific physical position on the CD surface, the computer drive can detect every reading error and track its original location simultaneously.

Several free CD-quality diagnostic programs, such as PlexTools Professional, Kprobe, and CD-DVD Speed were identified to be able to access the error-statistic information in a CD/DVD drive and to generate a plot displaying the variation of the block error rate as a function of playtime. Because the playtime of a digital audio file corresponds to a specific physical position on the CD surface, the location where the binding event occurred can be determined if it causes a significant disruption of the laser reading. For example, a typical 700-MB CD-R contains 79.7 min of audio data: if an error peak occurs at the playtime around the 15-min mark in the error distribution plot, the biomolecular binding event would take place at an approximate orbicular location with a radius of 33.77 mm, as calculated from the following equation,

$$r = \sqrt{\frac{t}{79.7}\left(58^2 - 25^2\right) + 25^2} \tag{3.1}$$

where *t* is the playtime (min) and *r* is the radius of the location (radial distance).

Based on the detection principle described above, the performance (lateral resolution and sensitivity) of this digital readout protocol was first evaluated by applying a series of microsize colour stains at different locations on the CD surface. As shown in Figure 3.3, these stains generated significant errors

when read by a standard optical drive, in contrast to the minimal errors shown in the bottom plot. It is evident that an object with a diameter larger than 260 μm can be recognized by an optical drive and that the block error rates depend on the darkness of each stain spot. The detection range of this reading program is between 10 and 300 errors/s (block error rate); below the lower limit, the signal is difficult to distinguish from the background, while over the upper limit, the detected signal will be saturated. The time needed to obtain the test results shown in Figure 3.3 is much shorter than the playtime of the audio tracks; for example, less than 92 s is required to examine an entire CD if a 52× optical drive is used for the detection.

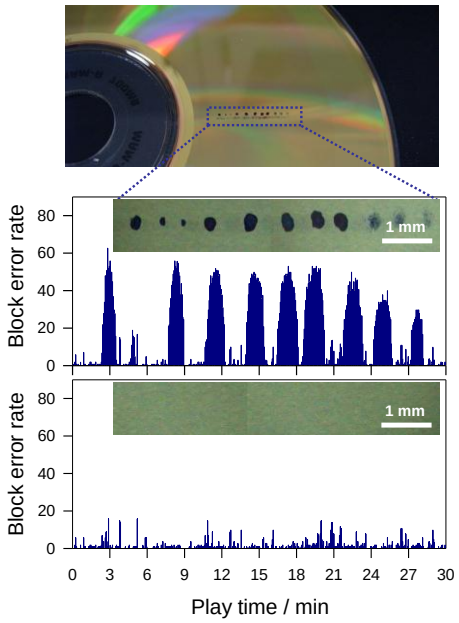

Figure 3.3. Optical image of a disc with colour stains and the corresponding reading error (block error rates) vs. radial distance (mm). The bottom plot shows the background error rate distribution before staining.

The successful detection of microsize features on the CD surface gave us the confidence to screen classical biomolecular interactions with this digital readout system. Biotin-streptavidin binding, one of the most frequently studied biological interactions, was the interaction examined. Five binding strips were formed on the PC surface of an audio CD-R with the assistance of PDMS plates. They were designed to test the binding of surface-bound biotin (prepared by coupling biotinyl-3,6,9-trioxaundecanediamine to carboxylic acid groups on an activated CD surface, Figure 3.1a) to five different concentrations of gold nanoparticle-streptavidin conjugate. To exclude potential contaminations from the multistep surface reaction, the diagnostic program was run to check the error distribution of the CD after each treatment. Upon the completion of the silver staining reaction, the CD exhibited a characteristic error distribution with five distinct peaks whose digital positions (playtime) perfectly matched the corresponding physical locations of the binding strips (Figure 3.4a). Atomic force microscopy (AFM) images (Figure 3.4b) revealed that they were composed of large-sized nanoparticles (~90-300 nm) with different particle densities (increasing gradually with increasing streptavidin concentration). The particle size variations are due to differences in the number of gold nanoparticle “seeds” and the effects of competitive growth. The data plotted in Figure 3.4c demonstrate that both the error rates and the optical darkness ratios (ODR) of the binding signals (determined with an optical microscope) depend on the target concentrations. The optical darkness ratio (ODR) is defined by eq. 3.2

$$\text{ODR} = \frac{\mathrm{I}_b - \mathrm{I}_s}{\mathrm{I}_b} \tag{3.2}$$

where I_b is the average luminosity of the background and I_s the value for the binding site, which is a function of particle size and density.[89] In the low target concentration range, error level and ODR are approximately proportional to the concentration of the target molecules (streptavidin); at higher concentrations, both reach a plateau due to signal saturation. This result not only validated the disc-based assay preparation and digital reading protocol but also laid the foundation for studying more complex bio-recognition reactions.

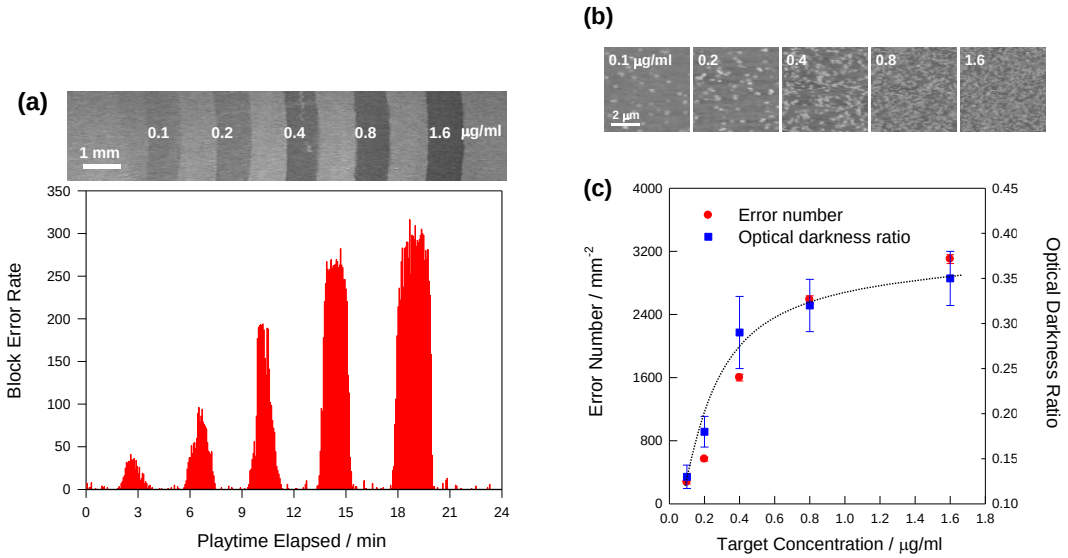

Figure 3.4. (a) Quantification of biotin/streptavidin binding assays; the distribution of block error rate on a CD modified with five strips of biotin/streptavidin binding lines. The top inset is an optical image of the binding strips. (b) AFM images of the binding strips to show the size and density of silver particles on the surface. (c) Relative error level intensity and optical darkness ratio as a function of the target concentration; the dashed line is to direct the eyes only. Three independent assay samples were used for the experimental uncertainty (error bar) determination in (c).

3.3.2.2 Reading Erroneous Bits

We also examined the feasibility of using a commercial CD-data analysis software (e.g., IsoBuster) in order to take a more direct approach quantifying

biochemical binding assays prepared on a disc. IsoBuster allows the detection to be more specific; it identifies the erroneous bits rather than the total error numbers per frame. The versatility of IsoBuster also provides the advantage of using any data format/media.

IsoBuster includes an option to create a list of all erroneous sectors of a file, track session or the entire medium, displaying only those that were truly read. The comprehensive procedure that we employed included a full surface scan followed by extraction of the raw data from an erroneous file. This flags the affected tracks as erroneous (Figure 3.5a). The figure shows five columns indicating the name of the track, logical block address (LBA), size of the track in localized bytes, size of the track in bytes and the date when the original track was written. The tracks affected by errors are marked with a red “X” symbol. Each group of Xs corresponds to an individual strip; due to the width of each strip, several tracks were affected when a binding strip was formed on CD. The software also lists the total number of errors occurred. For the disc tested with a target concentration range of 0.32 – 1.6 μg/mL, a total of 1508 erroneous sectors were detected (Figure 3.5b).

(a)

04 - MAROONED582.mp3	5167	5.01 MB	5,253,746	6/6/1999 6:48:38
04 - MAROONED583.mp3	7733	5.01 MB	5,253,746	6/6/1999 6:48:38
04 - MAROONED584.mp3	10299	5.01 MB	5,253,746	6/6/1999 6:48:38
04 - MAROONED585.mp3	12865	5.01 MB	5,253,746	6/6/1999 6:48:38
04 - MAROONED586.mp3	15431	5.01 MB	5,253,746	6/6/1999 6:48:38
04 - MAROONED587.mp3	17997	5.01 MB	5,253,746	6/6/1999 6:48:38
04 - MAROONED588.mp3	20563	5.01 MB	5,253,746	6/6/1999 6:48:38
04 - MAROONED589.mp3	23129	5.01 MB	5,253,746	6/6/1999 6:48:38
04 - MAROONED5810.mp3	25695	5.01 MB	5,253,746	6/6/1999 6:48:38
04 - MAROONED5811.mp3	28261	5.01 MB	5,253,746	6/6/1999 6:48:38
04 - MAROONED5812.mp3	30827	5.01 MB	5,253,746	6/6/1999 6:48:38
04 - MAROONED5813.mp3	33393	5.01 MB	5,253,746	6/6/1999 6:48:38
04 - MAROONED5814.mp3	35959	5.01 MB	5,253,746	6/6/1999 6:48:38
04 - MAROONED5815.mp3	38525	5.01 MB	5,253,746	6/6/1999 6:48:38
04 - MAROONED5816.mp3	41091	5.01 MB	5,253,746	6/6/1999 6:48:38
04 - MAROONED5817.mp3	43657	5.01 MB	5,253,746	6/6/1999 6:48:38
04 - MAROONED5818.mp3	46223	5.01 MB	5,253,746	6/6/1999 6:48:38
04 - MAROONED5819.mp3	48789	5.01 MB	5,253,746	6/6/1999 6:48:38
04 - MAROONED5820.mp3	51355	5.01 MB	5,253,746	6/6/1999 6:48:38
04 - MAROONED5821.mp3	53921	5.01 MB	5,253,746	6/6/1999 6:48:38
04 - MAROONED5822.mp3	56487	5.01 MB	5,253,746	6/6/1999 6:48:38

(b)

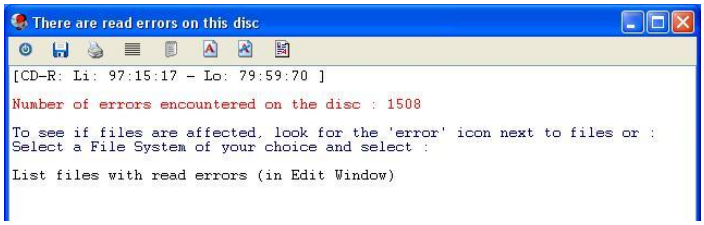

Figure 3.5. A sample report for a CD with a concentration range of 0.32 – 1.60 µg/ml. (a) Grouped errors detected by IsoBuster on three binding "strips". (b) Error report showing the total number of errors caused by all binding "strips."

To ascertain the exact number of sectors affected and their locations, the written tracks were subjected to an error extraction function. This function scans through the affected track and creates a list of erroneous sectors, and gives options of extracting the sectors with or without raw hexadecimal data. Particularly when the function encounters an erroneous sector, it allows four possible actions: (1) omit any substitution data of affected sector; (2) replace the entire sector with zeros while keeping the sector size intact. With this option the sector containing the original data affected with errors will be changed to zeros; (3) replace only user data in the sector affected with errors with zeroes, implying

that the raw data (sync bytes, headers, subheaders, etc.) are intact and the user data contain all zeroes; (4) replace the entire sector data including both the raw and user data with hexadecimal error/sense codes, which inform the host (computer and/or application) of an error situation. In our experiments, the option (4) was selected. As a verification step, the Sector View (showing hexadecimal data) of the erroneous sector and the sector with the same logical block address on the reference CD was compared and showed data change. Comparison of unaffected sectors on the CDs with biotin-streptavidin binding assays and the reference CD, having the same logical block address (LBA) showed no change in hexadecimal data.

The number of error sectors affected in a group (corresponding to a specific binding “strip”) and the concentration of streptavidin were plotted as shown in Figure 3.6. The graph shows a clear monotonic increase as the concentration of target streptavidin increases. This result was reproducible on independently prepared CDs with this trial binding assay.

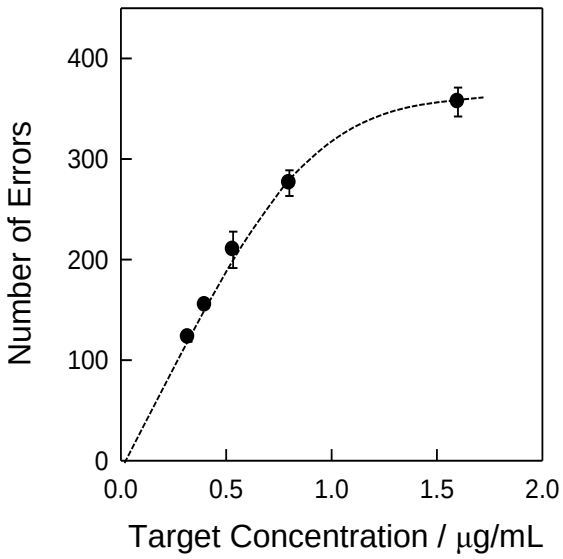

Figure 3.6. Number of error sectors versus concentration of streptavidin-gold nanoparticle conjugates. The concentration range is 0.32 – 1.6 μg/mL. The dashed line is to direct the eyes only. The error bars were determined from two independent discs.

In addition to the reading and quantifying biochemical binding assays prepared on a disc as provided by PlexTools Professional, the versatility of IsoBuster provides the advantage of using any data format/media. More importantly, IsoBuster allows the detection to be more specific; it identifies the erroneous bits rather than the total error numbers per frame. This provides the most “direct” approach to use consumer electronic products for biomedical diagnostics. Nonetheless, using IsoBuster can be more laborious. Whereas PlexTools Professional gives an error distribution plot in one click, Isobuster gives the number of errors in one sector and the total erroneous bits in a binding strip had to be calculated manually. Because PlexTools Professional was

sufficient in quantifying biomolecular binding events on discs, this diagnostic software was used for the remaining experiments.

3.4 Conclusion

A digital readout methodology, which is based on the reading-error determination principle of audio CDs, for screening biomolecular binding reactions has been developed. Using a standard computer drive without any modification to the hardware or control software, this novel signal-readout system "recognizes" staining spots larger than 260 μm on a CD surface. Bioassays can be prepared in simple array format with microfluidic equipment or tools. When read by a conventional optical drive, the error rate of pre-recorded audio files is a quantitative measure of the concentration of molecular analytes in the testing solution. In all cases, the readout error levels were found to be well-correlated with their ODR values. The CD-based readout system has a much higher sensitivity than the conventional fluorescence method, and it has the potential to screen a large number of binding assays on the same disk simultaneously.

4: APPLICATIONS OF THE DISC-BASED BIOASSAY TECHNIQUE

This chapter bridges the gap between the newly developed bioDisc technology and real-world applications. Using the disc-based bioassay technique, the detection and quantitation of the cancer marker CA215 have been demonstrated. Sandwich structures are commonly used in biomedical assays to improve the selectivity and sensitivity of the screening. RP215, an antibody specific for CA215, was used as both the capture and detection antibodies to prepare the sandwich assay on disc, followed by the silver-staining treatment to enhance the signal. It has been shown that the bioDisc technique can detect CA215 in physiological buffers at a concentration of 40 pg/ml, which is comparable to the standard, multistep ELISA assays (the detection limit is 30 pg/mL). Nonetheless, the bioDisc method effectively reduces the cost of biomedical tests. In addition, a lower detection limit can be obtained with further optimization.

4.1 Introduction

Being the leading cause of death worldwide, killing 7.4 million people in 2004,[90] cancer has been the one of the major health concerns in many parts of the world.[91] Despite the high cancer mortality each year, cancer is not at all incurable; the key to cure cancer is early detection, before its invasion of surrounding tissues or distant organs.[92] However, the common screening method

for cancer relies on an over-100-year-old method in which the pathologist inspects cell morphology by fixing tissues on paraffin.[1] In spite of the rapid advances in biotechnology and medical science, there is a clear need for diagnostic device improvement.[1]

Cancer markers are a result of abnormal cellular activities. Changes in gene sequences produce protein products that are different from those produced by normal cells. Because these altered protein products are generated in a higher rate or exclusively in cancer cells, they can be used to assess tumour burden (known as “cancer markers”). Depending on the type of markers, they can stay with the tumour or sloughed off the organ into body fluids such as blood plasma, urine, or saliva. Consequently, by monitoring their abundance in the patients’ body fluid, it is possible to monitor the progression of the cancer.[93]

CA215 is a generic cancer marker, first identified by Lee et al. at Vancouver Biotech Ltd.[94] Having a molecular weight of 60 kDa, CA215 has no light chains, in contrast to regular human immunoglobulins (IgG).[95] CA215 is either present on the surface of cancer cells or can be secreted into the surrounding area.[95] A high concentration of CA215 can be found in various types of cancer such as cervix, endometrium, esophagus, and ovary.[94] By immunizing mice with cell extracts of an ovary cancer cell line, fusing cells, and screening the resulting hybridomas, a monoclonal antibody designated as RP215 was developed.[96] It was found that the carbohydrate-associated epitopes of RP215 are located on the variable region of the immunoglobulin heavy chains of CA215.[97]

In this chapter, the sandwich assay structure used in ELISA will be adapted to the CD-based detection method for the quantification of the cancer marker CA215. The detection scheme is shown in Figure 4.1. The monoclonal antibody RP215 is the probe in this system, which is immobilized on the activated PC surface. After the addition of the analyte, CA215, the detecting antibody is introduced. The detecting antibody used here is also RP215, which can bind to CA215 at several different regions.[97] The detecting RP215 will be tagged with a biotin group, by which the streptavidin-nanogold conjugate-promoted silver staining protocol can be realized to enhance the binding signal.

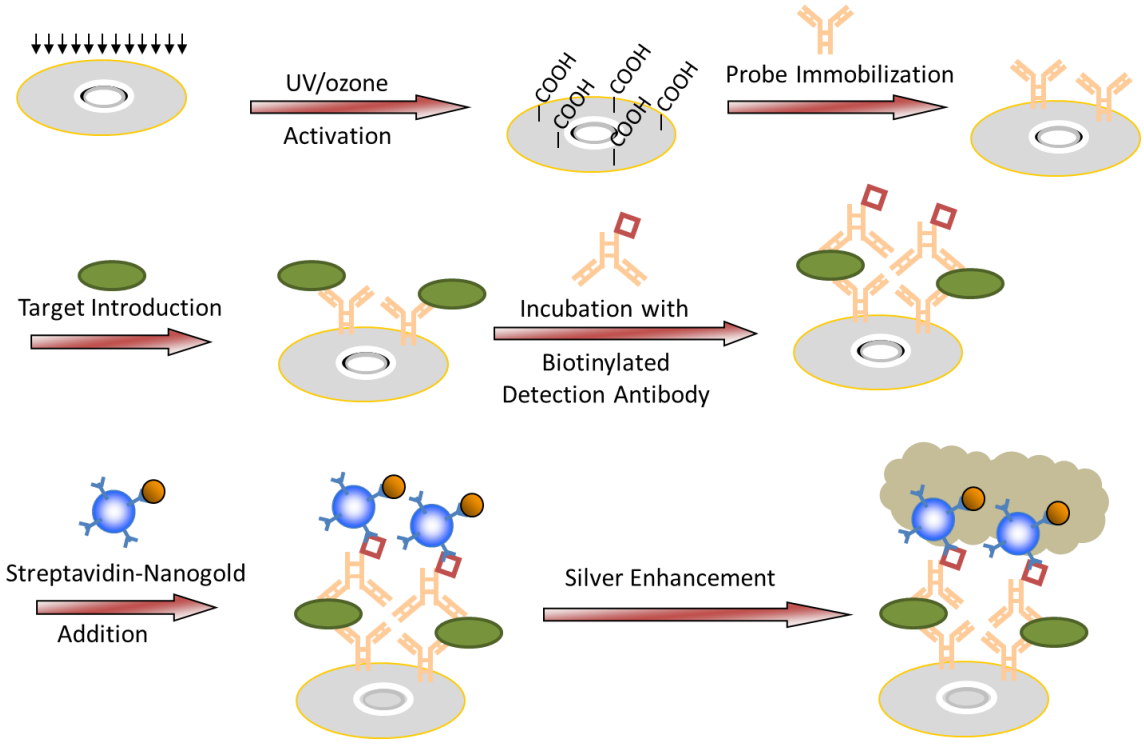

Figure 4.1. The detection scheme for CA215 on a bioDisc. After activating the PC with UV light in the presence of ozone, RP215 probes are immobilized on the CD surface. After addition of CA215 (analyte) and subsequently biotinlyated RP215 (detecting antibody), the introduction of streptavidin-nanogold conjugate and following silver enhancement allows the system to be amplified for screening with a standard computer drive.

4.2 Experimental Section

4.2.1 Biotinylation of RP215

Biotinylation of RP215 was performed using a biotin labelling kit (Dojindo Molecular Technologies, Inc.). Briefly, 100 μg of RP215 and NH_2-reactive biotin solutions were added to a filtration tube. After incubation at 37 ℃ for 10 min and centrifugation, the conjugate was recovered and stored at 4 ℃.

4.2.2 IgG/CA215 Detection

The disc was prepared and PC surface was activated as described in Section 3.4.1. To prepare an IgG indirect assay, human IgG (250 μg/mL) in 20 mM PBS-BSA buffer was allowed to react with the NHS-activated PC surface for 2 h at room temperature. The disc surface was then washed with phosphate buffer for 20 min, five concentrations of antihuman IgG solution (0.025, 0.05, 0.10, 0.25 and 1.0 μg/mL) were delivered, and the disc was incubated at room temperature for 90 min.

To prepare IgG/CA215 sandwich assays, upon treating the PC surface with EDC (100 mM) and NHS (25 mM) in the MES (0.1 M, pH 5.8) buffer for 3 h at room temperature, the surface was allowed to interact with 80 μL of probe molecules (anti-human IgG/RP215, 100 μg/mL) prepared in the immobilization buffer (10 mM phosphate, 150 mM NaCl, 5% glycerol, pH 7.4) overnight at 4°C. Probe solution on surface was confined in a PDMS micropool in a humid container (as mentioned in Chapter 2 and Chapter 3). After rinsing with PBS (20 mM phosphate and 150 mM NaCl at pH 7.4), the surface was blocked with BSA (20 mM phosphate, 150 mM NaCl, 4% BSA, and 2 mM NaN_3 at pH 7.4) at room temperature for 2 h. Another PDMS plate with microchannels was then sealed onto the reaction region. Each microchannels contained ~6 μL of solutions. Human IgG/CA215 of various concentrations prepared in the buffer (10 mM phosphate, 150 mM NaCl, 5% glycerol, pH 7.4) was introduced into the channels for incubation at room temperature for 1 h. After rinsing the channels with the PBS buffer, biotinlyated anti-human IgG/biotinylated RP215 prepared in 10 mM

phosphate, 125 mM NaCl, 5% glycerol, 0.1% BSA, and pH 7.4 (1 μg/mL) was then added to the channels at room temperature for 1 h. The channels were rinsed with the PBS buffer, followed by the addition of streptavidin-nanogold conjugate solution.

4.2.3 Signal Amplification and Signal Readout

Streptavidin-gold nanoparticle conjugates in the 20 mM phosphate buffer containing 0.8% BSA and 0.1% gelatin were added to bind to the biotin groups on the surface (middle panel of Figure 4.1). The CD was then rinsed sequentially with the phosphate buffer (20 mM phosphate, 150 mM NaCl, 5 min), deionized water (2 × 5 min), and 0.05 M EDTA at pH 4.5 (5 min). The removal of the PDMS stamp was followed by silver enhancement reaction; a mixture of equal volumes of the initiator and enhancer solutions provided by the manufacturer (Nanoprobes Inc.; LI Silver Kit) was introduced to the CD surface. Thus prepared bioDisc was then washed with deionized water, dried under nitrogen. A free diagnostic program (Plextools Professional LE V3.13 software, C1/C2 error test model, 10×24CAV) was then used to check the error distribution on the disc with a standard optical drive.

4.2.4 CA215 ELISA Test

The ELISA test was performed by following the instructions provided by the manufacture (VBL Serum CA215 EIA Test). Briefly, the CA215 standard (100 μL) was dispensed into the appropriate well, followed by the delivery of Enzyme Conjugate Reagent (50 μL) into the well. After one hour incubation, the mixture

was removed and the well was rinsed with 300 μL of the washing buffer (PBS) three times. The TMB solution (100 μL) was then added into the well. The reaction was stopped after 20 min by introducing 100 μL of Stop Solution. The signal was read with a microtiter well reader at 450 nm within 15 minutes.

4.3 Results and Discussion

4.3.1 Quantification of IgG using a Sandwich Assay

The quantification of IgG was first demonstrated to confirm the feasibility of the bioDisc technology in protein biomarker detection. In this assay, IgG was immobilized on the disc surface. The molecule being detected, biotinylated anti-IgG, was introduced from solution. The amount of binding between the two was quantified using the silver enhancement as described in the biotin-streptavidin test described in Ch. 3. In general, the immobilization of proteins is more challenging. Proteins are influenced by the temperature and pH easily and would lose activity as a result. Promising results (Figure 4.2) were obtained as indicated by the observed high detection sensitivity. The optical image and error distribution plots show that not only can a readable signal be obtained with a concentration as low as 25 ng/mL anti-IgG but also the saturation level is reached at a low concentration (250 ng/mL). The silver staining step required only 30 min to obtain sufficient contrast, which confirms the high efficiency of IgG immobilization and of anti-IgG binding.

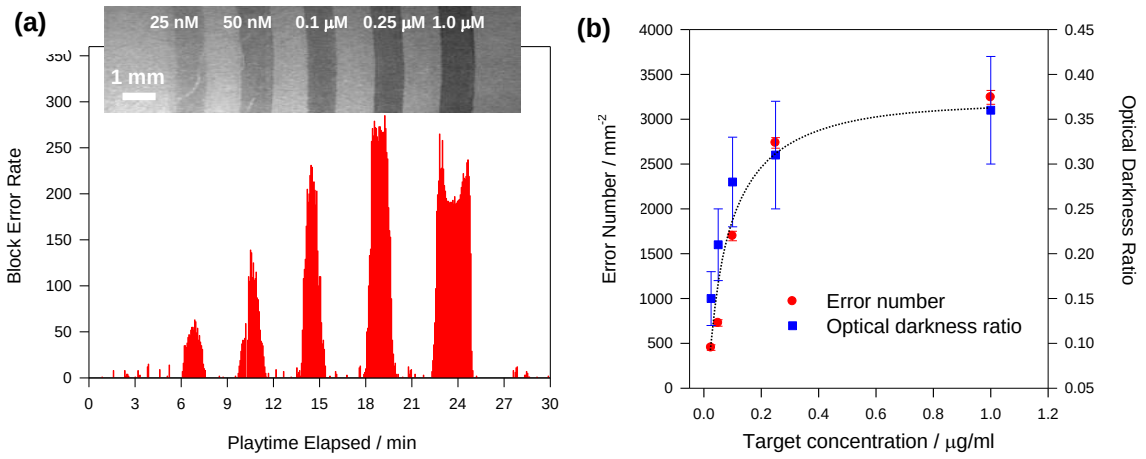

Figure 4.2. Quantification of human IgG/anti-human IgG binding assays on disc. (a) Block error rate distribution plot with an optical image at the top; (b) dependence of error levels and optical darkness ratios on the target concentrations. Three assay discs were examined to determine the experimental uncertainties shown in (b); the dashed line is to direct the eyes only.

As mentioned in the first chapter, the sandwich format for the detection of an analyte is usually preferred as compared to the indirect type because a reduced background signal would increase the sigal-to-noise ratio. To examine the feasibility of the sandwich structure, the interaction between human IgG and its counterpart anti-human IgG was investigated. In this case, anti-IgG was first immobilized on the disc surface. After introducing IgG, biotin-labelled anti-IgG was added to the system. The subsequent silver enhancement provided sufficient signal amplification to disrupt laser reading in the unmodified optical drive. Figure 4.3a shows a representative error distribution plot for the sandwich assay for the detection of IgG. As the laser scanned outward, the laser passed various silver strips where the reaction took place. The strips were intentionally arranged so that each strip represents a specific concentration of the analyte and

the concentration increased from innermost strip outward. The result shows a clear trend in which the number of erroneous frames per second increased as the playtime proceeds. By relating the physical location of the strip to its playtime using the formula (Eq. 3.1), each of the reaction strip can be “traced” to the concentration of the standard solutions. Based on the data shown in Figure 4.3a, a calibration curve is constructed by using the concentration of IgG and normalizing the signals with respect to the “strip” areas (Figure 4.3b). From the plot, even though the lowest obtainable signal is approximately the same (i.e. 25 ng/mL), the working range is significantly wider for the sandwich format. Instead of a saturation level of 250 ng/mL in the indirect method, the saturation level is reached at 2.5 μg/mL for the sandwich assay.

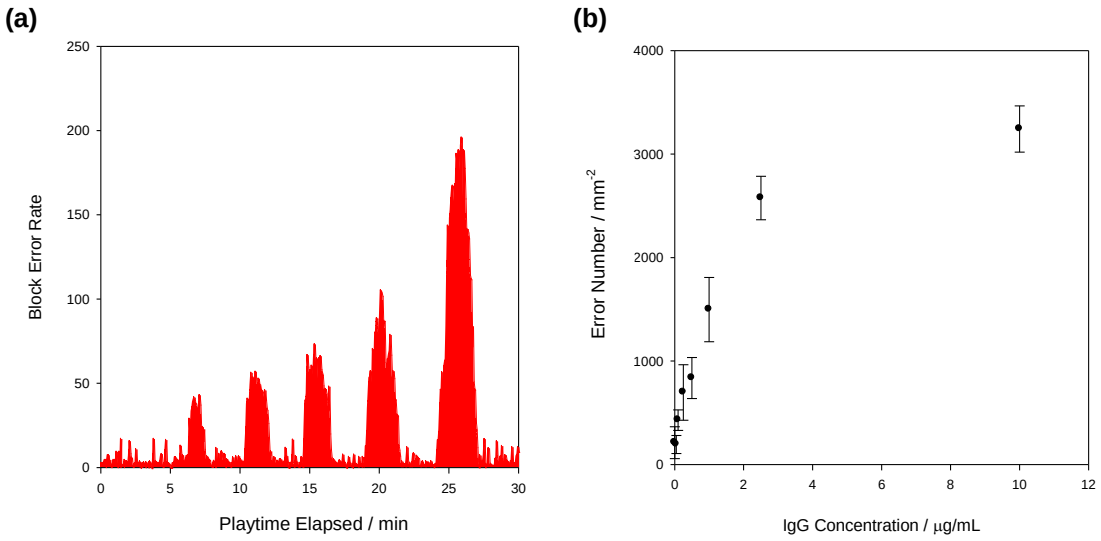

Figure 4.3. Quantification of human IgG by using a sandwich assay format. (a) Block error rate distribution plot; (b) dependence of the error levels on the target concentrations. Five assay discs were prepared to obtain the data points and experimental uncertainties in (b).

4.3.2 Detection of the Cancer Marker CA215

The current method used to quantify serum CA215 levels is the enzyme-linked immunosorbent assay (ELISA). In this specific assay, the plastic well is coated with RP215. After the introduction of a solution containing CA215, horseradish peroxidase (HRP)-linked RP215 is added into the well. The enzymatic reduction of H_2O_2 leads to the oxidation of a colourless substrate TMB (3, 3', 5, 5'-tetramethylbenzidine) to produce a coloured product on the surface (Scheme 4.1).[98,99] After the first oxidation step, a blue product which is a charge-transfer complex of the parent diamine and the diimine oxidation product exists in equilibrium with a radical cation. The second oxidation step yields a yellow diimine product, which is stable at low pH.[98] After terminating the enzymatic reaction using a hydrochloric acid stop solution, the yellow product had the absorbance read at 450 nm. The resulting working curve is shown in Figure 4.4. The detection limit of 30 pg/mL was calculated by plugging the absorbance of the blank plus three standard deviations back into the working curve.

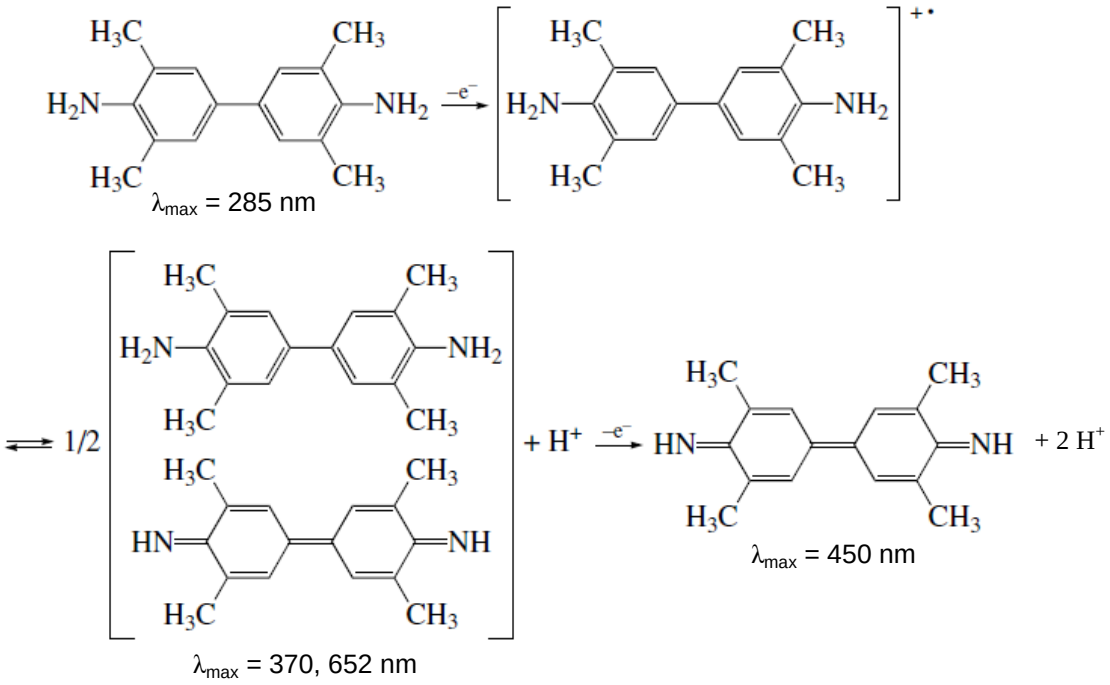

Scheme 4.1. The reaction scheme of peroxidase oxidation of TMB.[98,99]

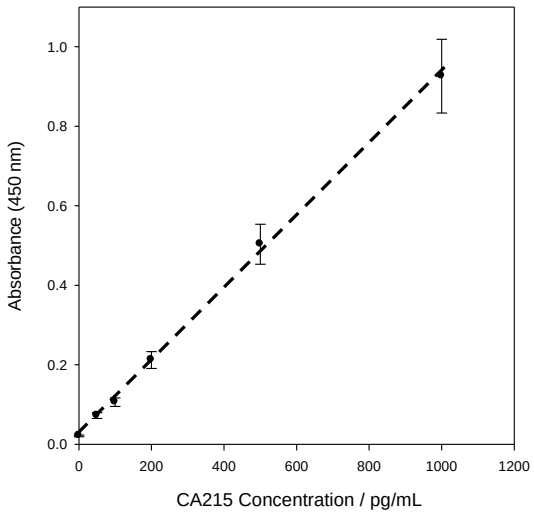

Figure 4.4. A representative plot with the absorbance taken at 450 nm. The dotted line is drawn to direct the eyes only. For each concentration, three different reaction wells on the plate were used for running the assay and for determining the experimental uncertainties.

The success in IgG quantification allowed us to go one step further, i.e., to detect the protein cancer marker, CA215, with the bioDisc technology. In this system, RP215 was used as the capture antibody and biotinylated RP215 as the detection antibody. Figure 4.5a shows a representative error distribution plot for the detection. Each peak corresponds to a specific concentration of CA215. After five trials and normalization, a calibration curve is constructed and shown in Figure 4.5b. A plot of error signals against the concentration yields a curve that has a linear range from 0 – 500 pg/mL.

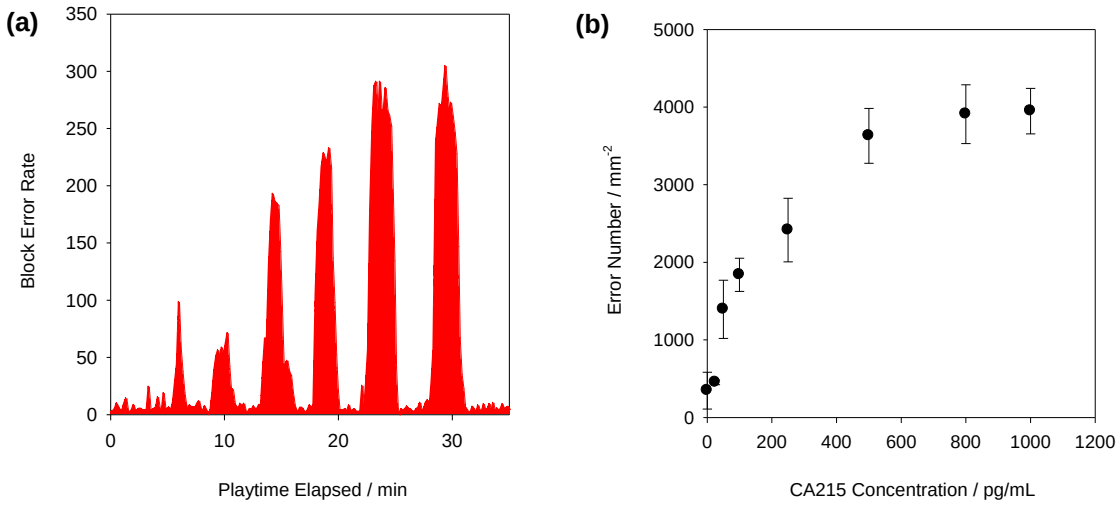

Figure 4.5. Quantification of CA215 by a sandwich assay. (a) Block error rate distribution plot; (b) dependence of error levels on the target concentrations. Data points and experimental uncertainties were obtained using the same way as specified in Figure 4.3.

The detection method was found to have a detection limit of 40 pg/mL, calculated as the mean background signal plus three standard deviations. The background signal was determined by using samples containing the buffer only and no CA215 was present. CA215 levels in cancer patients vary, with a minimum amount of 4 ng/mL.[100] Therefore, this method would be sufficient for CA215 level determination in patients.

4.3.2.1 Assay Specificity

Prior to the specificity test of the assay, the efficiency of the use of RP215 as the capture antibody was examined by replacing RP215 with mouse IgG. Instead of RP215, mouse IgG molecules were immobilized on the disc surface. Because mouse IgG has no affinity for CA215, there should not be any binding

between the two molecules. Consequently, no signal amplification should take place and laser scanning should not be disrupted. Figure 4.6 shows a typical error distribution plot, in which no distinguishable signal could be identified for analysis as expected.

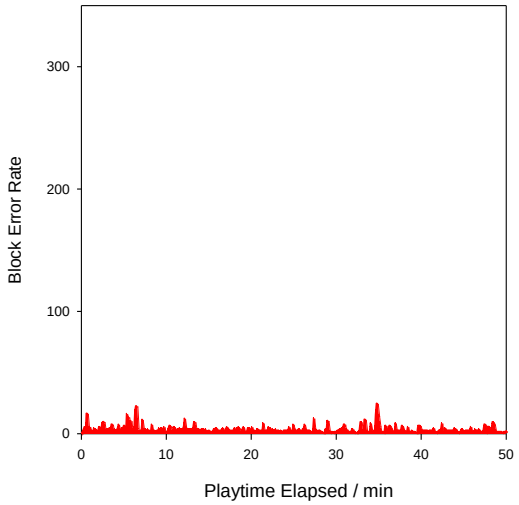

Figure 4.6. A typical error distribution plot for the capture antibody efficiency test in which mouse IgG was used instead of RP215.

The negative control test was performed by replacing the CA215 with its homolog, human IgG. After immobilizing RP215 on the PC surface, CA215, human IgG, and buffer-only solutions were introduced to corresponding channels. A concentration of 1000 pg/mL was used for the test. Biotinylated RP215 was used as the detection antibody and streptavidin-nanogold conjugate was added for silver enhancement. As shown in Figure 4.7, the signal for CA215 was significantly larger than the signal for human IgG, whereas the signal for the

buffer-only sample was not detectable. These results indicated that this sandwich assay was specific only to the desired analyte, CA215.

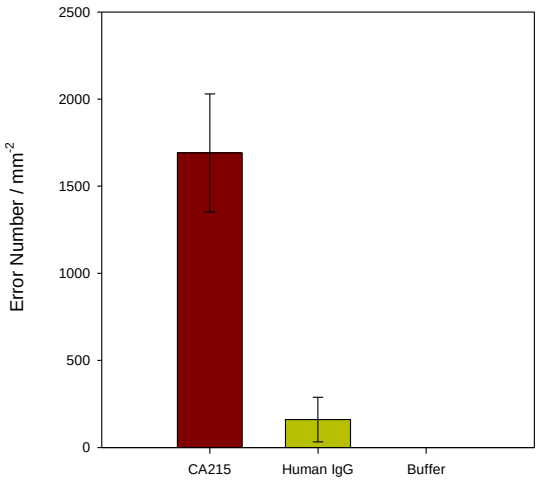

Figure 4.7. A comparison error plot for the assay specificity test in which CA215, human IgG, and buffer-only samples were used as the analytes. Each sample was repeated twice on an assay disc. Three independent assay discs were used to determine average error numbers and experimental uncertainties to construct the graph shown. The signal for CA215 was significantly larger than the signal for either human IgG or buffer-only samples.

4.4 Conclusion

In this chapter, the newly developed bioDisc technique was employed for the detection of CA215 (a generic cancer biomarker). By preparing a sandwich format assay on disc, a calibration curve constructed covers two orders of magnitude (10 – 1000 pg/mL) and a concentration as low as 40 pg/mL can be detected. On the other hand, the conventional detection method, the ELISA, has a detection limit of 30 pg/mL. With its portability and lower cost, this disc-based

technique can be applied to other types of medical diagnoses. In addition, further optimization of the test conditions would allow the sensitivity to be improved.

5: CONCLUSION AND FINAL REMARKS

5.1 Summary

In this thesis project, a disc-based detection method and its application have been explored. At first, a mild surface activation method for the PC substrate of CDs was developed. Particularly, PC substrates (e.g., plastic bases of CDs) can be readily converted to a novel polymeric platform for the fabrication of chip-based biosensing devices (DNA microarray as an example) by brief UV/ozone treatment. The method is rapid (less than 10 min), efficient (yielding a high surface density of COOH), and non-destructive (surface morphology is not altered). The fabrication procedure (activation, patterning, and coupling) is simple and effective, and hybridization is highly sensitive and selective.

In the subsequent chapter, a digital readout methodology for screening biomolecular binding reactions, which is based on the reading error determination principle of audio CDs, has been developed. Using a standard computer drive without any modification to the hardware or control software, this novel signal-readout system “recognizes” staining spots larger than 260 μm on a CD surface. When read by a conventional optical drive, the error rate of pre-recorded audio files is a quantitative measure of the concentration of molecular analytes in the testing solution. In all cases, the readout error levels were found to be well-correlated with their ODR (optical darkness ratio) values.

Finally, applications of this disc-based technique were exemplified in a cancer marker detection. CA215, a generic cancer marker, was explored as a model system to demonstrate the versatility of the disc-based detection technique for biomedical diagnosis. By forming a sandwich structure with RP215 antibodies, CA215 can be detected at a level of 40 pg/mL, which is comparable to the conventional ELISA test and is sufficiently sensitive for cancer marker screening in patients (> 4 ng/mL is considered positive).

5.2 Future Work

This disc-based detection method is still at its infancy; many aspects of it can be further improved. Because this novel signal-readout system recognizes binding spots larger than 260 μm on a CD surface and a CD has 33 mm of programmable area, it is possible to run at least 100 samples on the same disc. A multiplex bioassay thus designed allows different types of analytes to be tested simultaneously. CA215 is a generic cancer marker; by coupling CA215 to other types of cancer marker such as CA125, a cancer marker known for ovarian cancer, a more accurate and reliable cancer diagnosis kit can be developed for cancer prognosis and diagnosis.

In addition to the changes in the number of samples performed on the disc, the amplification step can be improved. The silver staining amplification is sensitive but many factors such as incubation time, temperature, and pH of the solutions can affect the extent of silver staining. The mechanism of silver staining can be studied in more detail or another amplification approach can be used to improve the current amplification step.

In the past few years, digital versatile discs (DVDs) and blu-ray discs are gradually replacing the conventional compact discs. DVDs and blu-ray discs have the same specifications as CDs; however, DVDs use a laser of 650 nm and blu-ray discs use a laser of 405 nm for retrieving data stored in the disc as opposed to 780 nm used for CDs. By using lasers of shorter wavelengths, DVDs and blu-ray discs allow for a smaller size of pits embedded in the disc, which in turn allow a larger amount of data stored in the discs. With shorter wavelengths on the polycarbonate surface, the laser beam is focused to the pit surface at a smaller size; the smallest particle size on the disc that would create an error in the reading process would be reduced. Consequently, the silver particles generated on the disc surface could be smaller. In other words, the error detection method would be even more sensitive with DVDs or blu-ray discs in theory. DVDs or blu-ray discs can certainly be used in the next stage of the project to make the detection more sensitive.

Other than biological applications, this disc-based detection method can also be applied to other aspects of life. For instance, it can be used to determine the lead content in environmental samples. In fact, preliminary research has been carried out in our laboratory.[101] After the Pb^{2+}-specific DNAzyme sensing construct is immobilized on a CD-R surface, the Pb^{2+} concentration can be determined by the diagnostic program that checks the error distribution on the CD. The reading errors increases monotonically over a wide range of Pb^{2+} concentrations (from 10 nM to 1 mM) and the selectivity is confirmed by testing several other divalent cations (Zn^{2+}, Ba^{2+}, Mg^{2+}, Ca^{2+}, Cu^{2+}, Hg^{2+}). More

importantly, this detection method offers a platform technology for the fabrication of DNAzyme sensors to analyze other metal ions because DNAzymes specific for Hg^{2+}, Cu^{2+}, UO^{2+} and Zn^{2+} have also been obtained by *in vitro* selection.[102] With the standard optical drive being the only instrument required, the cost of environmental sample analysis is significantly reduced. Despite the fact that digestion of the sample is still required,[103] this disc-based analytical method undoubtedly does aid in making the analysis more accessible to peripheral laboratories rather than central laboratories. In doing so, the time and cost for the test would be further reduced.

REFERENCES

1. Soper, S. A.; Brown, K.; Ellington, A.; Frazier, B.; Garcia-Manero, G.; Gau, V.; Gutman, S. I.; Hayes, D. F.; Korte, B.; Landers, J. L.; Larson, D.; Ligler, F.; Majumdar, A.; Mascini, M.; Nolte, D.; Rosenzweig, Z.; Wang, J.; Wilson, D. *Biosens. Bioelectron*. **2006**, *21*, 1932-1942.

2. Yeo, D. S. Y.; Panicker, R. C.; Tan, L.-P.; Yao, S. Q. *Comb. Chem. High Throughput Screening* **2004**, *7*, 213-221.

3. Templin, M. F.; Stoll, D.; Schrenk, M.; Traub, P. C.; Vohringer, C. F.; Joos, T. O. *Trends Biotechnol*. **2002**, *20*, 160-166.

4. Wilson, D. S.; Nock, S. *Angew. Chem. Int. Ed*. **2003**, *42*, 494-500.

5. Mathews, C. K.; van Holde, K. E.; Ahern, K. G. Immunological Methods. In *Biochemistry*; Roberts, B.; Weber, L.; Marsh, J., Eds.; Addison Wesley Longman, Inc. Benjamin/Cummings: San Francisco, 2000; 3rd edn., p. 253.

6. OneTouch UltraMini Blood Glucose Monitoring System Owner's Booklet. LifeScan, Inc., 2007.

7. Sharpless, G. Introduction to CD and CD-ROM. Deluxe Global Media Services Ltd., 2003; p. 8.

8. Pohlmann, K. C. The Compact Disc System. In *The Compact Disc Handbook*; Strawn, J.; Roads, C., Eds.; Oxford University Press: New York, 2001; 2nd edn., Chapter 3, p. 47-101.

9. Birkett, D. *J. Chem. Educ*. **2002**, *79*, 1081-1087.

10. Pohlmann, K. C. CD Player Design. In *The Compact Disc Handbook*; Strawn, J.; Roads, C., Eds.; Oxford University Press: New York, 2001; 2nd edn., Chapter 4, p. 103-166.

11. Sharpless, G. Introduction to CD and CD-ROM. Deluxe Global Media Services Ltd., 2003; p. 6.

12. Sharpless, G. Introduction to CD and CD-ROM. Deluxe Global Media Services Ltd., 2003; p. 10.

13. Lane, P. M.; Dommelen, R. V.; Cada, M. *IEEE Trans. Educ*. **2001**, *44*, 47-60.

14. Yu, H.-Z. *Chem. Commun*. **2004**, 2633-2636.

15. Ho, C.; Soolaman, D. M.; Yu, H.-Z. *Can. J. Chem*. **2005**, *83*, 403-412.

16. Templeton, C.; Wuelfing, W. P.; Murray, R. W. *Acc. Chem. Res*. **2000**, *33*, 27-36.

17. Finklea H. O.; Hanshew, D. D. *J. Am. Chem. Soc*. **1992**, *112*, 3173-3181.

18. Khoshtariya, D. E.; Wei, J.; Liu, H.; Yue, H.; Waldeck, D. H. *J. Am. Chem. Soc*. **2003**, *125*, 7704-7714.

19. Drummond, T. G.; Hill, M. G.; Barton, J. K. *Nat. Biotechnol*. **2003**, *21*, 1192-1199.

20. Vercoutere, W.; Akeson, M. *Curr. Opin. Chem. Biol*. **2002**, *6*, 816-822.

21. Fojta, M. *Electroanalysis*. **2002**, *14*, 1449-1463.

22. Angnes, L.; Richter, E. M.; Augelli, M. A.; Kume, G. H. *Anal. Chem*. **2000**, *72*, 5503-5506.

23. Richter, E. M.; Augelli, M. A.; Magarotto, S.; Angnes, L. *Electroanalysis* **2001**, *13*, 760-764.

24. Richter, E. M.; Augelli, M. A.; Kume, G. H.; Mioshi, R. N.; Angnes, L.; *Fresenius J. Anal. Chem.* **2000**, *366*, 444-448.

25. Munoz, R. A. A.; Matos, R. C.; Angnes, L. *J. Pharm. Sci*. **2001**, *90*, 1972-1977.

26. Daniel, D.; Gutz, I. G. R. *Electroanalysis* **2001**, *13*, 681-685.

27. Daniel, D.; Gutz, I. G. R. *Electrochem. Comm.* **2003**, *5*, 782-786.

28. Telleman, P. Introduction. In *Microsystem Engineering of Lab-on-a-chip Devices*; Geschke, O.; Klank, H.; Telleman, P., Eds.; Wiley-VCH Verlag GmbH & Co. KGaA: Weinheim, 2008; 2nd edn., Chapter 1, p. 1-7.

29. Gorkin, R.; Park, J.; Siegrist, J.; Amasia, M.; Lee, B. S.; Park, J.-M.; Kim, J.; Kim, H.; Madou, M.; Cho, Y.-K. *Lab Chip* **2010**, *10*, 1758-1773.

30. Madou, M.; Zoval, J.; Jia, G.; Kido, H.; Kim, J.; Kim, N. *Annu. Rev. Biomed. Eng*. **2006**, *8*, 601-628.

31. Lai, S.; Wang, S.; Luo, J.; Lee, L. J.; Yang, S.-T.; Madou, M. J. *Anal. Chem*. **2004**, *76*, 1832-1837.

32. Peytavi, R.; Raymond, F. R.; Gagne, D.; Picard, F. J.; Jia, G.; Zoval, J.; Madou, M.; Boissinot, K.; Boissinot, M.; Bissonnette, L.; Ouellette, M.; Bergeron, M. G. *Clin. Chem*. **2005**, *51*, 1836-1844.

33. Lovrinovic, M.; Niemeyer, C. M. *Angew. Chem., Int. Ed.* **2005**, *44*, 3179-3183.

34. Pirrung, M. *Angew. Chem., Int. Ed.* **2002**, *41*, 1276-1289.

35. Cheung, V. G.; Morley, M.; Aguilar, F.; Massimi, A.; Kucherlapat, R.; Childs, G. *Nat. Genet.* **1999**, *21*, 15-19.

36. Dubitsky, A.; Brown, J.; Brandwein, H. *BioTechniques* **1992**, *13*, 392-400.

37. De Paul, S. M.; Falconnet, D.; Pasche, S.; Textor, M.; Abel, A. P.; Kauffmann, E.; Liedtke, R.; Ehrat, M. *Anal. Chem.* **2005**, *77*, 5831-5838.

38. Johnson, P. A.; Gaspar, M. A.; Levicky, R. *J. Am. Chem. Soc.* **2004**, *126*, 9910-9911.

39. Liu, Y.; Ganser, D.; Schneider, A.; Liu, R.; Grodzinski, P.; Kroutchinina, N. *Anal. Chem*. **2001**, *73*, 4196-4201.

40. Liu, Y.; Rauch, C. B. *Anal. Biochem*. **2003**, *317*, 76-84.

41. Welle, A.; Gottwald, E. *Biomed. Microdevices* **2002**, *4*, 33-41.

42. McCarley, R. L.; Vaidya, B.; Wei, S.; Smith, A. F.; Patel, A. B.; Feng, J.; Murphy, M. C.; Soper, S. A. *J. Am. Chem. Soc*. **2005**, *127*, 842-843.

43. Situma, C.; Wang, Y.; Hupert, M.; Barany, F.; McCarley, R. L.; Soper, S. A. *Anal. Biochem*. **2005**, *340*, 123-135.

44. Wei, S.; Vaidya, B.; Patel, A. B.; Soper, S. A.; McCarley, R. L. *J. Phys. Chem. B* **2005**, *109*, 16988-16996.

45. Kimura, N. *Biochem. Biophys. Res. Commun*. **2006**, *347*, 477-484.

46. Xu, Y.; Vaidya, B.; Patel, A. B.; Ford, S. M.; McCarley, R. L.; Soper, S. A. *Anal. Chem*. **2003**, *75*, 2975-2984.

47. Ishida, T.; Hara, M.; Kojima, I.; Tsuneda, S.; Nishida, N.; Sasabe, H.; Knoll, W. *Langmuir* **1998**, *14*, 2092-2096.

48. Ponter, A. B.; Jones, Jr. W. R.; Jansen, R. H. *Polym. Eng. Sci.* **1994**, *34*, 1233-1238.

49. Wojtyk, J. T. C.; Tomietto, M.; Boukherroub, R.; Wayner, D. D. M. *J. Am. Chem. Soc.* **2001**, *123*, 1535-1536.

50. Delamarche, E.; Bernard, A.; Schmid, H.; Michel, B.; Biebuyck, H. *Science* **1997**, *276*, 779-781.

51. Delamarche, E.; Bernard, A.; Schmid, H.; Bietsch, A.; Michel, B.; Biebuyck, H. *J. Am. Chem. Soc.* **1998**, *120*, 500-508.

52. Duffy, D. C.; McDonald, J. C.; Schueller, O. J. A.; Whitesides, G. M. *Anal. Chem.* **1998**, *70*, 4974-4984.

53. Huang, Z.; Szostak, J. W. *Nucleic Acids Res.* **1996**, *24*, 4360-4361.

54. Fixe, F.; Dufva, M.; Telleman, P.; Christensen, C. B. V. *Nucleic Acids Res.* **2004**, *32*, e9 (1-8).

55. Holmes-Farley, S. R.; Reamey, R. H.; McCarthy, T. J.; Deutch, J.; Whitesides, G. M. *Langmuir* **1985**, *1*, 725-740.

56. Holmes-Farley, S. R.; Bain, C. D.; Whitesides, G. M. *Langmuir* **1988**, *4*, 921-937.

57. Liu, Y. J.; Navasero, N. M.; Yu, H. Z. *Langmuir* **2004**, *20*, 4039-4050.

58. Rivaton, A. Maihot, B.; Soulestin, J.; Varghese, H.; Gardette, J. L. *Polym. Degrad. Stab.* **2002**, *75*, 17-33.

59. Rivaton, A. *Polym. Degrad. Stab.* **1995**, *49*, 163-179.

60. Hillborg, H.; Tomczak, N.; Olah, A.; Schonherr, H.; Vancso, G. J. *Langmuir* **2004**, *20*, 785-794.

61. Diaz-Quijada, G.; Wayner, D. D. M. *Langmuir* **2004**, *20*, 9607-9611.

62. Teare, D. O. H.; Ton-That, C.; Bradley, R. H. *Surf. Interface Anal.* **2000**, *29*, 276-283.

63. Joos, B.; Kuster, H.; Cone R. *Anal. Biochem.* **1997**, *247*, 96-101.

64. Koch, C. A.; Li, P. C. H.; Utkhede, R. S. *Anal. Biochem.* **2005**, *342*, 93-102.

65. Lee, H. J.; Goodrich, T. T.; Corn, R. M. *Anal. Chem.* **2001**, *73*, 5525-5531.

66. Jia, G.; Ma, K.-S.; Kiod, H.; Zoval, J. V.; Madou, M. J. *Proc. NSTI-Nanotech* 2005; Vol. 1, pp 624-627.

67. Peng, X. Y.; Li, P. C. H.; Wang, L.; Yu, H. Z.; Parameswaran, M.; Chou, W. L. *Proceeding of the 9th International Conference on Miniaturized Systems for Chemistry and Life Sciences*; Boston, 2005; pp 823-825.

68. Schena, M.; Schalon, D.; Davis, R. W.; Brown, P. O. *Science* **1995**, *270*, 467-470.

69. Debouck, C.; Goodfellow, P. N. *Nat. Genet.* **1999**, *21*, 48-50.

70. Schweitzer, B.; Wiltshire, S.; Lambert, J.; O'Malley, S.; Kukanskis, K.; Zhudagger, Z.; Kingsmore, S. F.; LizardiDagger, P. M.; Warddagger, D. C. *Proc. Natl. Acad. Sci. U. S. A.* **2000**, *97*, 10113-10119.

71. Petrik, J. *Transfusion Med.* **2006**, *16*, 233-247.

72. Morais, S.; Marco-Moles, R.; Puchades, R.; Maquieira, A. *Chem. Commun.* **2006**, 2368-2370.

73. Li, Y.-C.; Wang, Z.; Ou, L. M. L.; Yu, H.-Z. *Anal. Chem.* **2007**, *79*, 426-433.

74. Varma, M. M.; Inerowicz, H. D.; Regnier, F. E.; Nolte, D. D. *Biosens. Bioelectron.* **2004**, *19*, 1371-1376.

75. Singh, B. K.; Hillier, A. C. *Anal. Chem*. **2006**, *78*, 2009-2018.

76. Madou, M. J.; Lee, L. J.; Daunert, S.; Lai, S.; Shih, C. H. *Biomed. Microdevices* **2001**, *3*, 245-254.

77. Alexander, I.; Houbion, Y.; Collet, J.; Hamels, S.; Demarteau, J.; Gala, J. L.; Remacle, J. *BioTechniques* **2002**, *33*, 435-439.

78. Barathur, R.; Bookout, J.; Sreevatsan, S.; Gordon, J.; Werner, M.; Thor, G.; Worthington, M. *Psychiatr. Genet*. **2002**, *12*, 193-206.

79. Lange, S. A.; Roth, G.; Wittemann, S.; Lacoste, T.; Vetter, A.; Grassle, J.; Kopta, S.; Kolleck, M.; Breitinger, B.; Wick, M.; Horber, J. K. H.; Dubel, S.; Bernard, A. *Angew. Chem. Int. Ed*. **2006**, *45*, 270-273.

80. Potyrailo, R. A.; Morris, W. G.; Leach, A. M.; Sivavec, T. M.; Wisnudel, M. B.; Boyette, S. *Anal. Chem*. **2006**, *78*, 5893-5899.

81. Banuls, M.-J.; Gonzlez-Pedro, V.; Puchades, R.; Maquieira, A. *Bioconjugate Chem*. **2007**, *18*, 1408-1414.

82. Morais, S.; Carrascosa, J.; Mira, D.; Puchades, R.; Maquieira, A. *Anal. Chem*. **2007**, *79*, 7628-7635.

83. La Clair, J. J.; Burkart, M. D. *Org. Biomol. Chem.* **2003**, *1*, 3244-3249.

84. La Clair, J. J.; Burkart, M. D. *Org. Biomol. Chem.* **2006**, *4*, 3052-3055.

85. Zhao, N.; Weng, L. H.; Zhang, X. Y.; Xie, Q. D.; Zhang, X. L.; Xu, J. *ChemPhysChem* **2006**, *7*, 824-827.

86. Jones, C. L. *Probl. Nonlinear Anal. Eng. Syst*. **2005**, *11*, 17-36.

87. Alexandre, I.; Hamels, S.; Dufour, S.; Collet, J.; Zammatteo, N.; De Longueville, F.; Gala, J.-L.; Remacle, J. *Anal. Biochem*. **2001**, *295*, 1-8.

88. Liang, R.-Q.; Tan, C.-Y.; Ruan, K.-C. *J. Immunol. Methods* **2004**, *285*, 157-163.

89. Gupta, S.; Huda, S.; Kilpatrick, P. K.; Velev, O. D. *Anal. Chem*. **2007**, *79*, 3810-3820.

90. Fact Sheet on Cancer. World Health Organization, 2009.

91. Jemal, A.; Siegel, R.; Ward, E.; Hao, Y.; Xu, J.; Murray, T.; Thun, M. J. *CA Cancer J. Clin.* **2008**, *58*, 71-96.

92. National Cancer Control Programmes Policies and Managerial Guidelines. World Health Organization, 2002; 2nd edn., Chapter 5, p. 55-68.

93. Sidransky, D. *Nature Rev. Cancer* **2002**, *2*, 210-219.

94. Lee, G.; Chu, R.-A.; Ting, H. H. *Cancer Biol. Ther.* **2009**, *8*, 161-166.

95. Lee, G.; Laflamme, E.; Chien, C.-H.; Ting, H. H. *Cancer Biol. Ther.* **2008**, *7*, 2007-2014.

96. Lee, G.; Ge, B. *Cancer Immunol. Immunother.* **2010**, *59*, 1347-1356.

97. Lee, G.; Ge, B. *Cancer Biomarkers* **2009**, *5*, 177-188.

98. Josephy, P. D.; Eling, T.; Mason, R. P. *J. Biol. Chem*. **1982**, *257*, 3669-3675.

99. Kireyko, A. V.; Veselova, I. A.; Shekhovtsova, T. N. *Russ. J. Bioorg. Chem*. **2006**, *32*, 71-77.

100. Lee, G.; Ge, B.; Huang, T.-K.; Zheng, G.; Duan, J.; Wang, I. H. Y. *Cancer Biomarkers* **2010**, *6*, 111-117.

101. Wang, H.; Ou, L. M. L.; Suo, Y.; Yu, H.-Z. *Anal. Chem*. **2011**, *83*, 1557-1563.

102. Lu, Y.; Liu, J.; Li, J.; Bruesehoff, P. J.; Pavot, C. M.-B.; Brown, A. K. *Biosens. Bioelectron.* **2003**, *18*, 529-540.

103. Pyle, S. M.; Nocerino, J. M. *Environ. Sci. Technol*. **1996**, *30*, 204-213.